THE EFFECT OF SOIL RESISTIVITY ON THE LV SURGE ENVIRONMENT

Shuxin Yang

A research report submitted to the Faculty of Engineering, University of the Witwatersrand, Johannesburg, in partial fulfilment of the requirements for the degree of Master of Science in Engineering.

Johannesburg, April 2006

DECLARATION

I declare that this research report is my own, unaided work, except where otherwise acknowledged. It is being submitted for the degree of Master of Science in Engineering in the University of the Witwatersrand, Johannesburg. It has not been submitted before for any degree or examination in any other university.

Signed this _____ day of _____ 20___

_____

Shuxin Yang

ABSTRACT

Due to the high soil resistivities and high frequency of lightning strikes in South Africa, the background theory about the effect of soil resistivity on the LV surge environment is important, but the present local and international standards do not give reasonable explanations for this effect. The previously published experimental results and research results related to this effect were investigated. From these investigations, it can be shown that the soil resistivity can affect surge generation, surge propagation and surge attenuation significantly. Also, soil resistivity plays a main role in the lightning surges caused by both direct strikes and indirect strikes, which can cause severe damage to the LV distribution system. Soil resistivity also has a significant impact on the resistance of an earth electrode.

ACKNOWLEDGEMENTS

I would like to acknowledge the supervision and guidance given by my colleagues in the HV LAB of Wits University throughout the duration of the research.

I would also like to thank all my friends in South Africa.

A special thanks goes to my family for their continual support and encouragement.

CONTENTS

LIST OF FIGURES

LIST OF TABLES

Chapter 1

INTRODUCTION

Many local and international standards covering surge protection and the lightning protection have been issued. The principles of design, installation, inspection, and maintenance of surge and lightning protection systems are described in detail in SABS IEC 1024(1990), SABS IEC 61312(1995), SABS IEC 61643(1998) and SABS 0313(1999). The measurement of soil resistivity and the methods of reducing soil resistivity are introduced. The transient impedance characteristics are mentioned in SABS 0199-1985. IEC 62305-2(2005) is applicable to the decision on whether SPDs (Surge Protective Devices) and other protection measures need to be adopted. Soil resistivity is a factor in procedure for risk assessment but the reasoning is not explained.

In South Africa, most consumers live in areas characterized by dry, sandy or rocky soil, where the soil resistivities are high. Therefore the effect of soil resistivity on the LV surge environment is important.

In order to provide the background theory about the effect of soil resistivity on the LV surge environment, and compile a document that is useful to another project (serving for IEC 62305-2) that investigating the risk issues related to the surge environment in domestic premises, this research report will focus on the papers and literature which have been published about the effect of soil resistivity on the LV surge environment. The effect of soil resistivity on the process of surge generation, surge propagation and surge attenuation will be highlighted.

In this research report, many papers that have been published will be referred to, some of the authors who have contributed research on the effect of soil resistivity are: R. Rudenberg. (1945) Korsuncev, A.V.(1958), Liew, A. C. & Darveniza, M. (1974), William. C. J. Blattner (1982), Oettle, E. E. (1987), A. Chisholm & Wasyl. Janischewskyj (1989), Abdul.M. Mousa (1994), Y L Chow, M M Elsherbiny, M M A

Salama (1996), Rhett Alexander Kelly (1996), Nixon, Kenneth John (1999), Carlos T. Mata, Mark I. Fernandez, Vladimir A.Rakov, Martin A. Uman (2000), Carlo Alberto Nucci, Silva Guerrieri, M. Teresa Correia de Barros, and Farhad Rachidi (2000), Adam Semlyen (2002), JM Van Coller (2004).

The structure of the research report is as follows:

Chapter 2 introduces the general structure of MV/LV distribution systems, the frequency of lightning and the soil characteristics in South Africa. The earthing standards are presented as well.

Chapter 3 describes natural and external factors affecting soil resistivity. It also introduces methods to reduce soil resistivity and methods to test soil resistivity in different soil conditions.

Chapter 4 introduces the types of surges and the effect of surges on the power network. Lightning surges are highlighted. It also describes the effect of ground conductivity on lightning electromagnetic fields.

Chapter 5 introduces the process of surge propagation and the factors affecting it. It also presents the model of transmission lines used to show the effect of soil resistivity. A theoretical analysis and formulation on the influence of ground conductivity on lighting-induced voltages on an overhead wire are presented.

Chapter 6 introduces the possible approaches for attenuating surges and the effect of soil resistivity on surge attenuation. The forms of earth electrodes and related models are analyzed specifically, and the effects of soil ionizations are also included.

Chapter 7 provides the conclusions of this research report.

Chapter 2

BACKGROUND

This chapter introduces the general structure of MV/LV distribution systems, the frequency of lightning and the soil characteristics in South Africa. The earthing standards are presented.

2.1 LV Power Supply Topology of South Africa

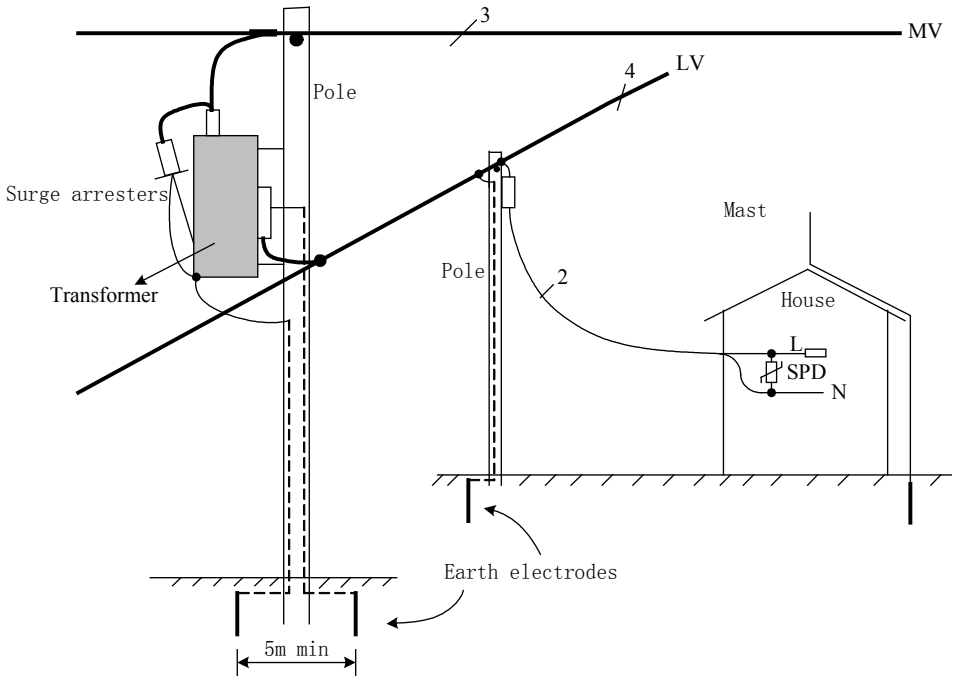

Fig 2.1 Simplified layout of the LV distribution system

In South Africa, a general LV distribution system is illustrated in Fig 2.1 above. The LV supply cable is fed from a pole mounted MV/LV distribution transformer. The transformer is supplied off an overhead 22kV MV reticulation network. Three separate, unshielded, bare, overhead conductors are the preferred means of MV reticulation. Electricity dispensers are installed at each customer, together with small power

distribution boards which are supplied via a single-phase concentric cable. Each service cable is fed off one phase of a three-phase LV overhead cable or buried cable.

The transformer is protected against surges on the MV system by MV surge arresters connected between the MV phases and the transformer tank. The transformer tank is connected to the MV earthing system. The LV neutral of the transformer is connected to an LV earth electrode.

2.2 Frequency of Lightning in South Africa

It is important to know how often lightning flashes occur in South Africa in order to research the effect of lightning. One way of representing this is in the form of the lightning ground flash density N_g, which is the number of cloud-to-ground flashes per square kilometer per year. In terms to SABS 0313 (1999)[7] the average annual lightning ground flash density for areas in South Africa are shown in Table 2.1.

Table 2.1 Lightning ground flash density N_g

Location	$N_g\left(flashes/km^2/year\right)$
Giant's Castle	13.0
Piet Retief	11.7
Carolina	9.0
Johannesburg and Pretoria	7.5
Bergville	6.3
Bloemfontein	5.2
Durban	5.0
Pietersburg	3.6
Port Elizabeth	0.9
Cape Town	0.3

2.3 The Characteristics of Soil in South Africa

In South Africa, most residences are located in areas characterized by dry, sandy or rocky soil. The prevailing values of soil resistivity are high and typically up to 2000 Ω m.

The identification of soil types at proposed sites for electrode installations can provide a useful indicator as to the expected value of soil resistivity. The typical soil resistivity values of some types of soils are shown in Table 2.2 [9].

Table 2.2 Typical soil resistivity values of some kinds of soils

Type of soil	Typical resistivity in Ω m		
Loams, garden soils	5	to	50
Clays	8	to	50
Clay, sand & gravel mixtures	40	to	250
Sand & gravel	60	to	100
Slates, shale & sandstone	10	to	500
Crystalline rocks	200	to	10000

2.4 Earthing Standards

For earthing systems, generally a low earth resistance is recommended (< 10 Ω)[32], four types of earth electrodes can be identified.

- Ring trench earth
- Driven vertical rods
- Radial electrodes

- Foundation electrodes/reinforcing conductors

The size of a conductor used for the earth electrode has no significant effect on it's resistance to earth. A solid Φ4mm copper conductor is preferred because it has greater mechanical strength and is less susceptible to corrosion. A buried earthing conductor and earth rods shall be at least 0.5 m below surface. The reason for this specification is that the layer of soil above the conductor forms an important medium into which the electrode can dissipate current. Deeply buried electrodes also exhibit less steep voltage gradients at the soil surface during times of current discharge. Further, deep burial reduces the possibility of mechanical damage of the earth electrode.

With reference to Fig 2.1, the MV earthing electrode should be placed as close to the transformer tank as possible in order that any surges on the MV system are transferred to ground by the shortest path. This will reduce the potential rise of the transformer tank and hence limit the inducted potential on the LV side. A low value of MV electrode resistance is to limit the current that can pass through any LV surge arrester.

For both 22 kV and 11 kV MV systems, the maximum allowable resistance of the transformer MV earth electrode is 30 Ω [9]. The three point star in Table 2.3 can be selected as the electrode configuration for the transformer MV earth electrode [9].

The separation between the MV and LV earth electrodes must be at least 5m in order to prevent MV earth faults affecting the LV system. The conductors connecting the earth rods shall be insulated over the full distance between electrodes. MV and LV earth electrodes may not be combined unless the total resistance of the combined electrode to remote earth is less than 1 ohm [9].

Table 2.3 Standard earth electrode configurations for 30 Ω resistances.

Electrode type	1	2	3	4	5	6
Electrode configuration	Three point star					
Soil resistivity	ρ = 300	ρ = 600	ρ = 900		ρ = 1500	
Number of rods	4	7	7	1	7	1
Diagrammatic represenation	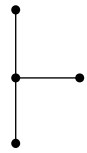	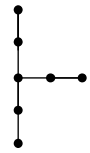	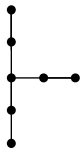	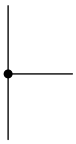	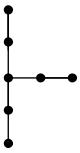	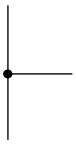

Single driven earth electrodes should be chosen for house earthing. In South Africa the Code of Practice for the Wiring of Premises (SANS 10142) does not require a local earth electrode. Thus the neutral is only earthed back at the MV/LV transformer.

For surge arrester mounted on a transformer earthing, the earthing system consists of a multiple rod electrode (preferably a three point star) with all connections being made and bonded to the main earthing lead.

Chapter 3

SOIL RESISTIVITY

This chapter describes the natural and external factors affecting soil resistivity. It also introduces methods to reduce soil resistivity and the methods to test soil resistivity in different soil conditions.

3.1 Definition

In SABS 0199-1985 [4], soil resistivity is defined as the resistance between the opposite faces of a cube of soil having sides of length 1m. Soil resistivity is expressed in ohm meters.

3.2 The Nature of Soil Resistivity

It is well known that the resistance of an electrode to earth is influenced by the resistivity of the surrounding soil. In a rural point of supply from a single transformer installation, a soil resistivity survey is required to establish the location best suited and most practically feasible for the transformer installation. The results are also used to select an earth electrode suitable for those specific soil conditions. To establish a network of transformer installations in urban areas, a separate soil resistivity survey should be conducted at each proposed location for a transformer installation. These results are used to select for each transformer an earth electrode that is suitable for the specific soil conditions at the equipment location [9].

The resistivity of soil is dependent on its composition and moisture content. These factors show wide variance from place to place and over time. The resistivity of the soil surrounding an earth electrode has a significant impact on the resistance of an earth electrode. Soil resistivity also has a bearing on the potential gradients that are to be

expected at the soil surface during times of fault current discharge through the earth electrode.

When the voltage developed at an earth electrode is high enough due to the injection of a large transient current, the surrounding soil will ionize, extending to some radial distance from the electrode surface.

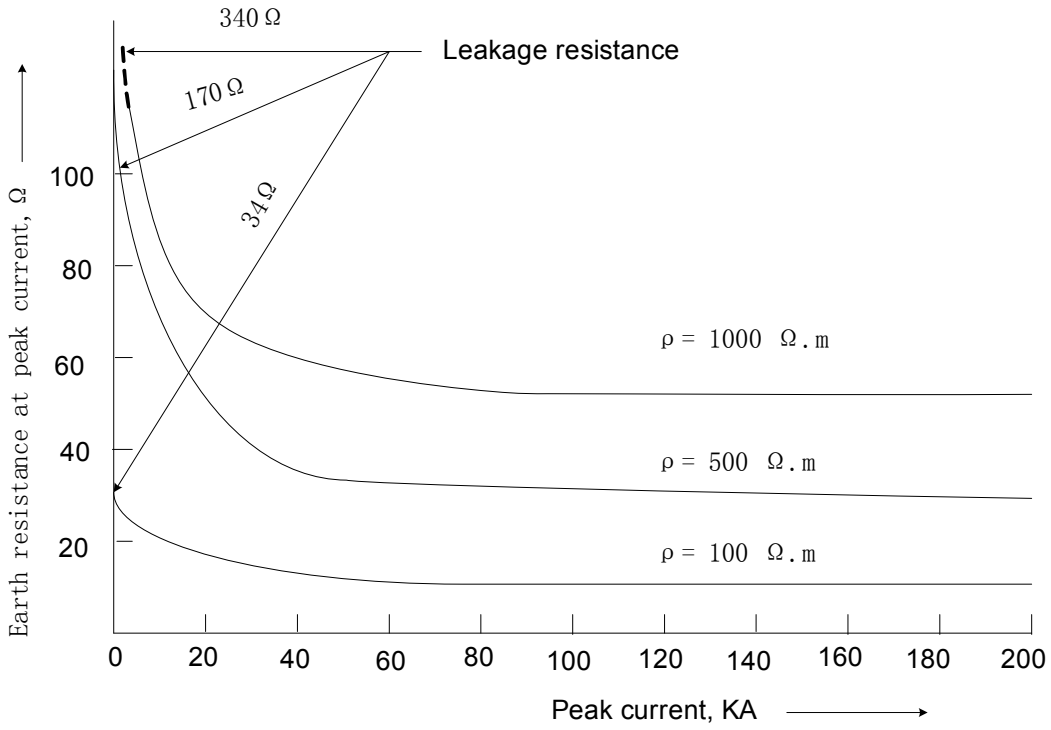

Fig 3.1 Decrease in earth resistance from the steady-state leakage resistance of a single driven rod resulting from ionization of the surrounding soil, as a function of impulse current

The effect of this envelope of ionized soil surrounding an electrode is to increase the effective radius thereby reducing the impedance of the earth electrode. It is clearly shown in Fig 3.1 that the difference between the low current resistance and the minimum dynamic resistance during ionization is quite marked and is typically between 20% and

80% [4]. For increasing resistivities the difference between the minimum resistance and the low current resistance, even at low current magnitudes, is noticeable.

Ionization plays an important role in limiting the absolute rise in surge potential of an earth electrode during the injection of lightning discharge currents.

3.3 Factors Affecting Soil Resistivity

3.3.1 Natural Factors

The oil is not a homogenous medium because of the variation of water content and also because of the variation in grain size and the existence of organic and man-made debris. However, in calculating the impedance of an earth electrode, we always assume that the soil is a homogenous medium and hence the formula would take simple forms which are easy to analyze. Under laboratory conditions, samples are made of sifted material and the water in the sample is reasonably well-mixed. As a result, the current becomes concentrated along several discrete channels and the assumed uniform shape of the ionized zone does not materialize.

The resistivity of soil varies with the depth from the surface, with the moisture content, and with the temperature of soil. The presence of surface water does not necessarily indicate low resistivity.

3.3.2 Driven Rod

When a rod or a pipe is driven in the ground, the electrode makes room for itself by compressing the soil in its immediate vicinity. This may affect the resistivity as well as the breakdown gradient at the surface of the electrode. This change is expected to be limited to a small soil volume around the electrode, typically a layer having a thickness equal to about twice the radius of the electrode.

3.3.3 Soil Ionization

During soil ionization, where a voltage peak leads a current peak, the soil ionization causes the effective resistance of a driven rod to drop to 17% of its low current resistance. This converts the affected portion of the soil from an insulator to a conductor, and is equivalent to a decrease in soil resistivity or an increase in the dimensions of the electrode when the soil was ionized.

Two different mechanisms have been suggested for the breakdown of the soil when it is subjected to a high voltage. One proposed explanation is that the initiation process is primarily electrical and the initiation begins when the electric field in the voids between the soil grains becomes large enough to ionize the air in the voids. Another proposed explanation is that the initiation mechanism is primarily thermal. But the evidence supporting the theory of breakdown by ionization of the air in the voids of the soil is quite convincing and is summarized by Mousa [15]. The most important proof is that Leadon et al. did tests in which the air in the voids was replaced by SF6; a gas that has a higher breakdown gradient. This resulted in an increase in the breakdown gradient of the soil, thus proving that breakdown is initiated by ionization of the gas in the voids.

3.4 The Methods of Reducing Soil Resistivity [4]

The artificial treatment of soil in the immediate vicinity of an electrode may lead to a significant decrease in local resistivity. Earth resistivity is particularly dependent upon moisture content and ionizable salt content. The usual methods for reducing earth resistivity involve increased water retention or chemical salting or both.

3.4.1 Watering of the Soil

Moist soil tends to have a reduced earth resistivity. Surface drainage systems can be channeled to maintain moisture in the soil in the vicinity of an electrode system. Unless

the watering of an electrode can be depended upon at all times, this method may not be sufficiently reliable.

3.4.2 Chemical Treatment

Treating the soil surrounding an electrode with a chemical does not necessarily reduce electrode resistance on a permanent basis since rainfall and natural drainage may gradually wash the chemicals out of the soil. It can be expected that these materials will need to be replenished at intervals of 2-3 years.

- Salt treatment

  In an area of high soil resistivity the earth resistance can be reduced by the application of salt in a water solution to the soil surrounding the electrode.

- Gel treatment

  Electrolytes mixed with the soil and that react to form a colloidal mass have a high conductivity. The potential gradients in the vicinity of an earth electrode may be reduced by saturating the surface soil with the gel.

- Special clay

  In an excavated earthing system, particularly if the soil is very sandy or is a gravel, a neutralized clay or a clay that has the property to absorbing water and swelling up to form a colloidal type material which fills the spaces between particles of sand or gravel can be used.

- Coke

  For the purpose of reducing the earth resistance, particularly in cathodic protection systems, crushed coke, having a particle size not exceeding 1-2mm, in the proportion by mass of one part of coke to four parts of soil can be used.

- Concrete encasement

  Concrete is inherently alkaline and hygroscopic. Its resistivity depends on the moisture content and may vary from 30-300 Ω m. Certain non-corrosive additives may further reduce the resistivity of the concrete.

3.5 The Methods of Soil Resistivity Measurement

3.5.1 Wenner Method

A practical method to determine the resistivity variation of the earth for the purpose of designing an earthing system is the four-electrode electrical sounding method. The most commonly used electrical sounding arrays are the Schlumberger and the Wenner arrays.
The Schlumberger method is recommended in all cases where accurate information on the resistivity, depth and number of layers is required and where depths greater than 20 m have to be investigated. The only advantage of the Wenner method is that a larger potential is measured and that less emphasis is therefore placed on the sensitivity of the measuring equipment.

By Wenner array [4], the apparent resistivity ρ_a , in ohm meters, is given by

$$\rho_a = K\frac{V}{I} = KR_m \tag{3.1}$$

Where $K = 2\pi a$ (a= probe spacing, m)
V = measured potential difference, V
I = measured current, A
R_m = measured apparent resistance, Ω

In most cases this method will be sufficient to assume a two-layer combination of earth of different resistivities.

3.5.2 Blattner Methods

Blattner [17] obtains soil resistivity based on three significantly different soil conditions: uniform soil, decreasing soil resistivity with depth and increasing soil resistivity with depth. The test methods are the apparent soil resistivity of a driven ground rod and the four-point method.

The four point measurements were conducted based on the Wenner four-electrode method.

$$\rho_W = 2\pi S R_W \tag{3.2}$$

Where ρ_W = average soil resistivity to depth S (Ω m)

S = spacing of electrodes (m)

R_W = measured value of resistance (Ω)

The driven rod apparent soil resistivity measurements were obtained by the simplified fall-of-potential method and calculated from the following equation:

$$\rho_D = \frac{2\pi L R_D}{\ln\frac{8L}{d} - 1} \tag{3.3}$$

Where ρ_D = apparent soil resistivity to depth L (Ω m)

L = length of driven rod in contact with earth (m)

d = diameter of rod (m)

R_D = measured value of resistance (Ω)

From the test results Blattner found that for uniform soil conditions, the two methods would yield essentially identical results, for non-uniform soil conditions, the two test

methods would yield significantly different results. It is apparent that the driven rod test results are significantly influenced by the layer of lowest resistivity.

To obtain an insight into the behavior of the test methods in non-uniform conditions, a theoretical analysis is made based on a two-layer soil condition.

- Driven rod test method

  A vertical driven rod installed in two layer soil as shown in Fig 3.2.

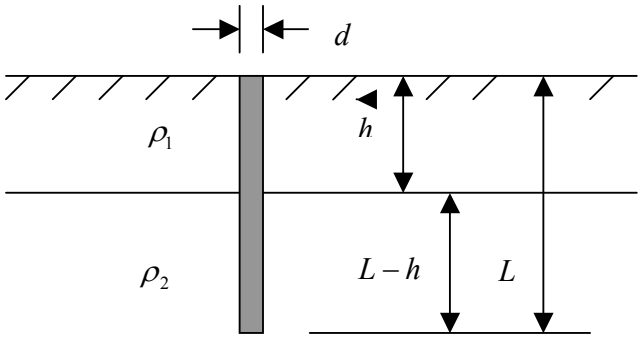

Figure 3.2 Driven rod in two layer soil

When a current I is injected into the rod shown above, the resulting current densities along the rod will be a function of the soil resistivities ρ_1 and ρ_2. The total current in the rod can be expressed as:

$$I = j_1 h + j_2 (L - h) \tag{3.4}$$

Where j_1 = current density in the rod part in ρ_1

j_2 = current density in the rod part in ρ_2

The apparent soil resistivity ρ_D can be expressed as:

$$\begin{aligned}\rho_D &= \frac{2\pi L R_D}{\ln\frac{8L}{d}-1} \\ &= \frac{2\pi L}{\ln\frac{8L}{d}-1}\left[\frac{\ln\frac{8L}{d}-1}{2\pi}\left(\frac{1}{\frac{h}{\rho_1}+\frac{L-h}{\rho_2}}\right)\right] \\ &= \frac{L\rho_1\rho_2}{\rho_2 h+\rho_1(L-h)}\end{aligned} \tag{3.5}$$

- Four point test method

  The principle of the four point method for uniform soil is developed, in terms of the potential difference between the potential probes. The same methodology is used herein to develop the potential difference between the potential probes in two layer soil conditions.

  Consider the four point test arrangement in Fig 3.3, where the top layer ρ_1 is shown as hemispherical shells around the current probes 1 and 2. For the purposes of this analysis the top layer thickness h is limited to the probe spacing S or less (h $\leqslant$ S).

  The potential difference between potential probe 3 and 4 is:

$$\begin{aligned}V &= V_3 - V_4 \\ &= \frac{I\rho_2}{2\pi(2S)} - \left(-\frac{I\rho_2}{2\pi(2S)}\right) \\ &= \frac{I\rho_2}{2\pi S}\end{aligned} \tag{3.6}$$

  The "measured resistance" R_W is:

$$
\begin{aligned}
R_W &= \frac{V}{I} \\
&= \frac{\rho_2}{2\pi S}
\end{aligned}
\tag{3.7}
$$

The "measured soil resistivity" ρ_W is:

$$
\begin{aligned}
\rho_W &= 2\pi S R_W \\
&= 2\pi S\left(\frac{\rho_2}{2\pi S}\right) \\
&= \rho_2
\end{aligned}
\tag{3.8}
$$

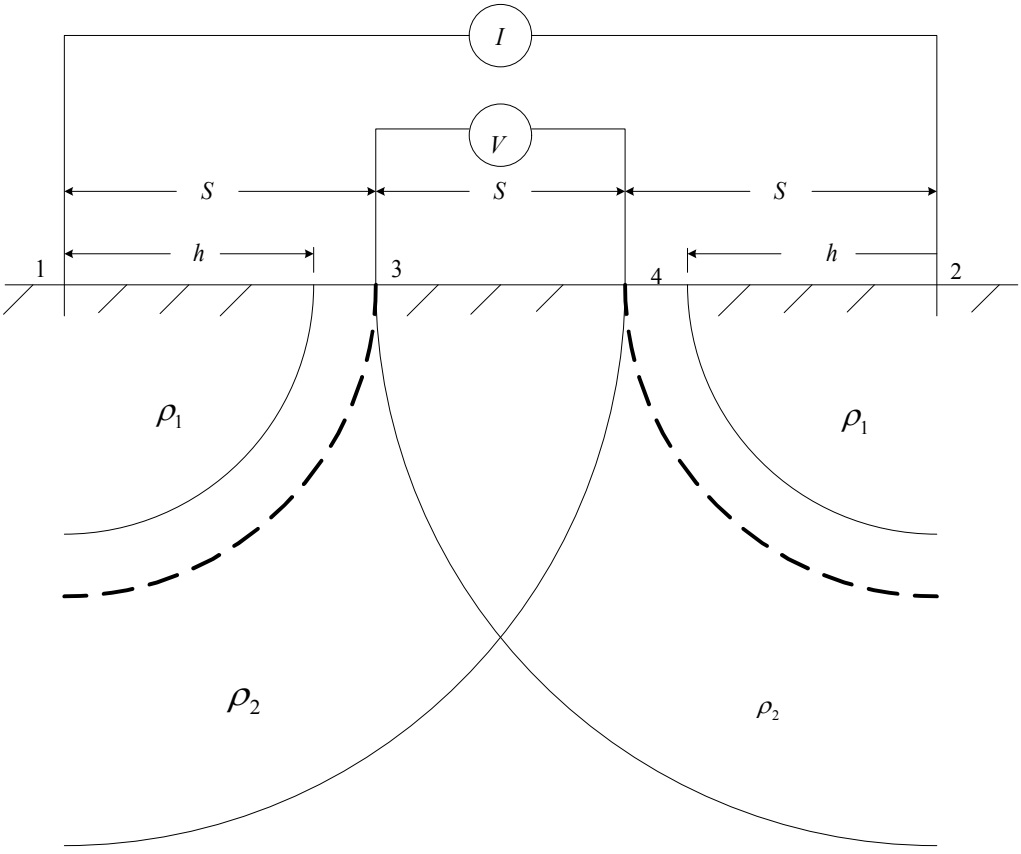

Fig 3.3 Four point test method

The above analysis is based on the condition h ≤ S. For the condition where the top layer thickness is greater than S, but less than 2S (S < h < 2S) the same methodology indicates a transition in measured values from ρ_2 to ρ_1. For the condition where h is equal to or greater than 2S (h≥ 2S) , the measured values reflect only ρ_1.

Blattner [23] also introduced another method of prediction of soil resistivity based on the fact that the test ground rods always were driven to a depth of only two or three meters before a layer of rock was encountered. In this situation, the top layer of soil has a relatively high value of resistivity, as a result, the designer must consider the options of installing an extensive ground system utilizing the known soil conditions of the top layer of soil or he can consider the probable effectiveness of installing a deep ground electrode. He recommended an equation to predict the soil resistivity and ground rod resistance for deep ground electrodes as follows:

$$\rho_X = \rho_0 - k_\rho (b + \ln X) \tag{3.9}$$

Where ρ_X = soil resistivity to be determined at a depth L_X

ρ_0 = known value of soil resistivity at a depth L_0 ($L_X > L_0$)

k_ρ = soil resistivity constant

$$b = \left[\frac{\rho_2 \times R_0 \times 1.6}{\rho_0 \times R_2} \right]^a$$

ρ_2 = known value of soil resistivity at a depth greater than L_0

R_0 = known value of rod resistance at a depth L_0

R_2 = known value of rod resistance at same depth as ρ_2

$a = \pm 1$

$= +1$ if ρ_2 is less than ρ_0 ($\rho_2 < \rho_0$)

$= -1$ if ρ_2 is greater than ρ_0 ($\rho_2 > \rho_0$)

X = distance in meters between L_X and L_0

This equation has been verified by actual values tested, but the limitation of this technique is that the accuracy of the predictions is greatly affected by the rate of change of the soil resistivity over the reading obtained with the preliminary test ground rods. If the rate of change per meter is relatively constant, the more likely the projection will be accurate.

3.5.3 Analysis of the Results of the Measurements

If the resistivity is found to increase rapidly with increase of depth, one may deduce that there are deep layers of soil having a higher resistivity than that at the surface. A very rapid increase may indicate the presence of rock. In this case it could be difficult to install a vertical earth electrode and a horizontal electrode type should be considered. If the resistivity decreases rapidly with increased depth, the conclusion can be drawn that the deeper layers of soil have a lower resistivity and advantage will be gained by installing a deep earth electrode.

3.6 The Effect of Soil Resistivity in IEC62305-2

3.6.1 Derivation of Electric Field in Soil

When lightning strikes ground current density will be produced around the strike point in the soil. The formula [59] below shows an electric field E developed in homogenous ground by a current I flowing in soil with resistivity ρ at a distance r from a lightning strike.

$$E = \frac{I \cdot \rho}{2\pi r^2} \tag{3.10}$$

3.6.2 Collection Area of Flashes Striking the Service

Soil resistivity enters into the calculation of risk in IEC62305-2 through collection area A_l of flashes striking the service and collection area A_i of flashes to ground near the service. The difference between A_l and A_i is shown in Fig 3.4 [5].

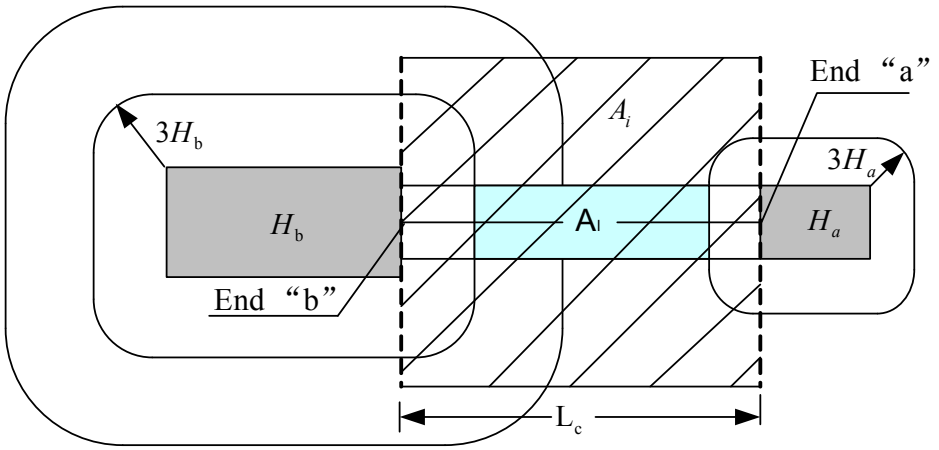

Figure 3.4 Collection area A_l of flashes striking the service and collection area A_i of flashes to ground near the service.

In calculating collection area A_l of flashes striking the service, the equation depending on the characteristics of buried service is shown:

$$A_l = \left(L_c - 3\left(H_a + H_b\right)\right)\sqrt{\rho} \tag{3.11}$$

Where

L_c is the height of the service section from the structure to the first node (m). In terms of the definition of node, node is a point on a service line at which surge propagation can be assumed to be neglected. Nodes can be a point on a power line branch distribution at a HV/LV transformer, a multiplexer on a telecommunication line or SPD installed along the line. Generally nodes of service are located at the entrance of the structure. The length between a structure and an adjacent node is less than 1000m.

Therefore, for the purpose of calculation a maximum value L_c = 1000m should be assumed.

H_a is the height of the structure connected at end "a" of service (m); end "a" can be seen as a node of service connected to the structure.

H_b is the height of the structure connected at end "b" of service (m); end "b" can be seen as a node of service connected to the structure.

ρ is the resistivity of soil where the service is buried (Ω m). As shown in table 2.2, except Crystalline rocks, the typical soil resistivity values of the most kinds of soils are less than 500 Ω m, such as sand, gravel, slate, shale and sandstone. Therefore for the purpose of calculation a maximum value ρ = 500 Ω m should be assumed.

From the equation 3.13 we can see that $\sqrt{\rho}$ can be assumed as the width of Collection area A_l

3.6.3 Collection Area of Flashes to Ground near the Service

In calculating collection area of flashes to ground near the service A_i, the equation depending on the service characteristics for buried cables is shown:

$$A_i = 25 L_c \sqrt{\rho} \tag{3.12}$$

where

L_c is the height of the service section from the structure to the first node (m). As equation 3.10 a maximum value L_c = 1000m should be assumed.

ρ is the resistivity of soil where the service is buried (m). As equation 3.13 a maximum value ρ = 500 Ω m should be assumed.

From the equation 3.14 we can not see the meaning of $\sqrt{\rho}$, probably the same assumption was made as equation 3.13.

3.6.4 The Relationship between Electric Field and Soil Resistivity

When lightning strikes ground adjacent to cable, due to the cable is straight line the area around the cable can be considered as collection area A_l and A_i in Figure 3.4. If we extend the area πr^2 of equation 3.12 to collection area A_l and A_i, the new equations between electric field and soil resistivity can be derived as.

- For collection area A_l of lightning flashes striking the service.

$$\begin{aligned} E_l &= \frac{I \cdot \rho}{2\pi r^2} \\ &= \frac{I \cdot \rho}{2} \frac{1}{(L_c - 3(H_a + H_b))\sqrt{\rho}} \\ &= \frac{I \cdot \sqrt{\rho}}{2(L_c - 3(H_a + H_b))} \end{aligned} \tag{3.13}$$

- For collection area A_i of lightning flashes to ground near the service.

$$\begin{aligned} E_i &= \frac{I \cdot \rho}{2\pi r^2} \\ &= \frac{I \cdot \rho}{2} \frac{1}{25 L_c \sqrt{\rho}} \\ &= \frac{I \cdot \sqrt{\rho}}{50 L_c} \end{aligned} \tag{3.14}$$

Analyzing the equation 3.15 and 3.16 we can find that electric field adjacent to the cable is proportional to the square root of the soil resistivity.

Chapter 4

SURGE GENERATION

This chapter introduces the types of surges and the effect of surges on the power networks. Lightning surges are highlighted due to their significant effect on the power networks. It also describes the effect of ground conductivity on lightning electromagnetic fields.

4.1 Introduction to Surges

Surge overvoltages are caused by lightning discharges, switching operations in electrical circuits, and electrostatic discharges. Surges typically have durations from microseconds to milliseconds. Nevertheless, these voltages, which are usually very high, are capable of destroying power systems or electronic circuits.

4.2 The Types of Surges

Surges on LV power networks may be generally identified as being either system-generated (internal overvoltage surges) or externally-generated (lightning overvoltage surges)

4.2.1 System Overvoltages

4.2.1.1 Power Frequency Overvoltages

During earth faults healthy phases can rise to high voltages. The main causes of temporary 50 Hz overvoltages are

- Disconnection of inductive loads.

- Connection of capacitive loads

- Unbalanced ground faults

Power frequency faults are generally divided into two types – “direct short” and “ground fault”. A direct short can be caused by a phase-to-phase connection, also referred to as “line to line”. A phase-to-neutral connection can also be considered a direct short. Direct-shorts cause the largest fault current to flow. Ground faults occur when a phase conductor is connected to ground. It can be an accidental connection between a phase conductor and any grounded surface, such as a grounded metal enclosure. A ground fault will cause about 75% as much fault current to flow as a direct short. When a ground fault occurs, the equipment grounding conductor serves a very important function. It furnishes a low-impedance path for the fault current and causes the circuit overcurrent protective device to operate, thereby limiting the fault duration [38].

An overload occurs when electrical equipment or a conductor is operated in excess of its rated current. If an overload continues to exist for a period of time, damage can be done and a fault can take place.

4.2.1.2 Switching Surges

Switching surges are generated by the operation of circuit breakers and the inception of faults

Normal switching operations in a distribution system can cause overvoltage surges. These are generally not more than three times normal voltage and are of short duration. Overcurrent devices such as circuit breakers or fuses, in general, interrupt a circuit at a normal current level at which time the stored energy in the inductance of the circuit is zero. The overvoltages thus developed result from transient oscillation in the circuit capacitance and inductance, there being stored energy in the circuit capacitance at the time of current interruption.

Switching surges are of particular interest at the higher voltage levels because of

- The nonlinear behavior of the switching impulse strength of airgaps with increasing gap length

- The lower airgap strength for waveforms corresponding to that of switching surges

In terms of IEC 71-1, the double exponential switching impulse (250/2500 μ s) is shown in Fig 4.1 [36].

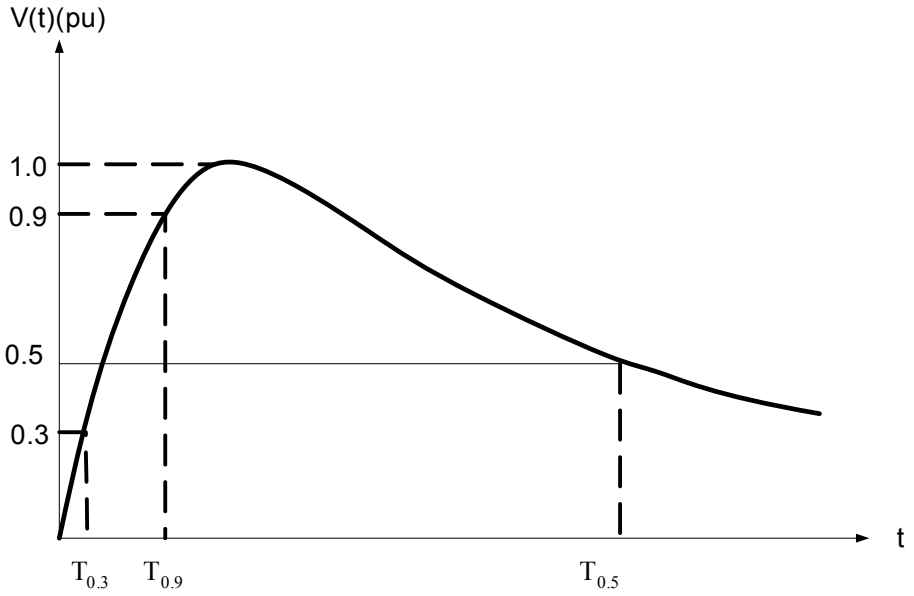

Fig 4.1Double exponential switching impulse

$$1.67\left(T_{0.9} - T_{0.3}\right) = 250\mu s \tag{4.1}$$

$$T_{0.5} = 2500\mu s \tag{4.2}$$

50Hz overvoltages usually occur together with switching surges so that surge arresters after operating during a switching surge must recover sufficiently to sustain the 50 Hz overvoltages.

4.2.1.3 Harmonic Overvoltage Surges

Main causes of temporary harmonic overvoltages are

- Disconnection of shunt compensated transmission lines (trapped charge oscillates between the line capacitance and the reactor inductance)
- Oscillation excited by the magnetizing current of unloaded transformers
- Resonance of series capacitance and lightly loaded transformer or shunt reactor
- Ferroresonance

4.2.2 Lightning Surges

Lightning surges can be generated on electrical distribution systems in several ways. Both MV and LV systems can be affected by direct and indirect lightning strikes.

4.2.2.1 The Mechanism of Lightning [32]

Lightning consists of the ionization of air, therefore providing a path for charge to flow. The leader breakdown mechanism is caused by the accumulation of a large amount of charge at a point within the cloud. When the electric field is high enough to cause electrical breakdown of the air, the air is ionized in narrow paths along which the charge moves. This charge is known as the stepped leader. The stepped leader creates a path along which more charge originating from the cloud can move. A large charge then accumulates at the end of the leader and the air around the tip is ionized and the process

repeats itself. Therefore as the stepped leader progresses, it leaves an ionized path containing charge behind it. A number of leaders could branch off in different directions resulting in the tree-like structure often observed in lightning.

Lightning is an ionized channel that propagates from one charge region to another oppositely charged region. Lightning discharges can be divided into two types:

- Cloud-to-ground discharges which have at least one channel connecting the cloud to the ground

- Cloud discharges that have no channel to ground. These cloud discharges can, in turn, be classified as in-cloud, cloud-to-air, and cloud-to-cloud.

For cloud-to-cloud lightning, the initiating and terminating charge regions are both in a thundercloud, while for cloud-to-ground lightning the initiating charge region is in a thundercloud and the terminating charge region is on the ground. Cloud-to-ground lightning normally has four types: negative downward, positive downward, positive upward and negative upward, the negative downward type is shown in Fig 4.2.

Lightning strokes from cloud to ground account only for about 10 percent of lightning discharges; the majority of discharges during thunderstorms take place between clouds. Discharges within clouds often provide general illumination.

4.2.2.2 Classification of Lightning Strikes

Lightning surges occur on LV power network in two ways: direct strikes to overhead conductors and electromagnetic coupling from nearby strokes.

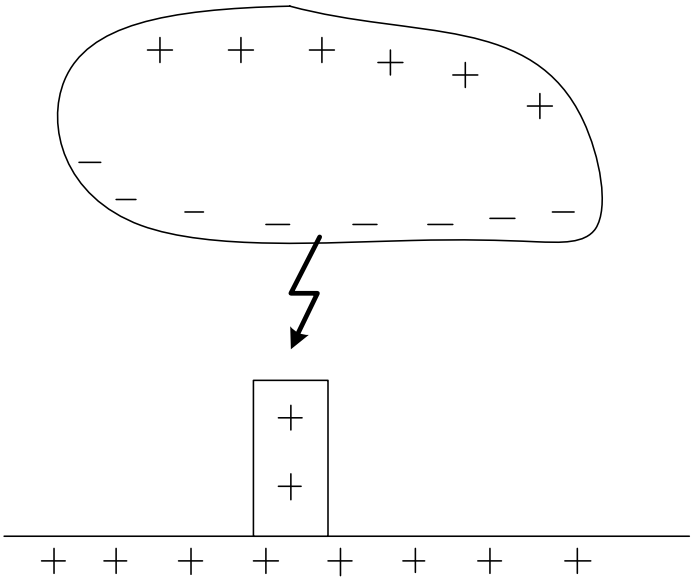

Fig 4.2 Negative downward type of cloud-to-ground lightning

4.2.2.2.1 Direct Strike

Direct strikes may occur to medium voltage lines with coupling through the distribution transformer to overhead LV conductors, direct strikes may also occur to low voltages line or to a building earth termination system.

4.2.2.2.2 Indirect Strike

Electromagnetic coupling may occur from strikes to nearby objects. Strikes to earth induce surges on buried cables and couple with adjacent conductors. Induced surges have lower peak current and voltage magnitudes than those caused by direct strikes.

Induced surges on power lines associated with adjacent lightning strikes are common mode (the same for each phase conductor) and hence the associated stress is between all three phases and ground rather than between the respective phases. Although lightning current is predominantly negative, induced voltages are usually positive with a rise time matching that of the current in the first stroke. Induced surges typically range from tens

of kilovolts to hundreds of kilovolts and seldom exceed 300kV. The MV line BIL(i.e. 300kV) is designed to limit the number of flashover due to indirect strikes.

When transient current flows in one of the adjacent cables – due to a direct strike or coupled current on an incoming conductor, whenever two cables run alongside each other, there must be inevitable interference that caused by electric field coupling and magnetic field coupling. The former coupling is caused by stray capacitance between the cables, while the latter is caused by the source cable acting as the primary winding of a transformer and the additional cable as a secondary winding. A shield wire does not protect against flashover during direct strikes. Shield wires reduce the induced voltages during adjacent strikes.

Large transient magnetic and electric fields are produced which will cause currents to flow in adjacent conductors, which may cause damage or upset to equipment connected to those conductors. A similar situation also exists for system-generated transients.

4.2.2.3 Lightning Strike Parameters

Lightning strokes are described in terms of their peak current, rise and fall times, charge content, rate of current rise and polarity. These parameters vary greatly with geographical location.

The double exponential lightning impulse (1.2/50 μ s) is shown in Fig 4.1 as well, and the parameters are:

$$1.67\left(T_{0.9} - T_{0.3}\right) = 1.2\mu s \tag{4.3}$$

$$T_{0.5} = 50\mu s \tag{4.4}$$

The following values should be compared with the standard waveforms used for testing electrical equipment:

1.2/50 μs (voltage)

8/20 μs (current)

The first stroke within a flash usually has the largest peak current , therefore when describing the peak current of a flash we usually imply that of the first stroke. The important peak current values of lightning strokes in terms of the probability of the peak current exceeding a particular value from SABS IEC 1024-1-1 (1993) [45] are shown in Table 4.1.

Table 4.1 Lightning current parameters – cumulative frequency distribution

	Cumulative frequency				
	98%	95%	80%	50%	5%
First negative stroke	4 kA		20 kA		90 Ka
Subsequent stroke		4.6 kA		12 kA	30 kA
Positive stroke		4.6 kA		35 kA	250 kA

SABS IEC 1312-1 (1995) recommends for design purposes the lightning current parameters of the first stroke in Table 4.2 [2].

Table 4.2 Lightning current parameters of the first stroke

Current parameters	Protection level		
	Ⅰ	Ⅱ	Ⅲ – Ⅳ
Peak current I (kA)	200	150	100
Front time T_1 (μs)	10	10	10
Time to half value T_2 (μs)	350	350	350
Charge of the short duration stroke Q_s (C)	100	75	50
Specific energy W/R (MJ/Ω)	10	5.6	2.5

Lightning and temporary overvoltages are the major influence factors in distribution networks, switching surges are less important. Therefore, in this research report, lightning surges will play a major role in describes the effect of soil resistivity on the LV surge environment.

4.3 The Effect of Surges on the Power Network

Lightning is often the cause of severe damage to structures due to direct strikes. Lightning is also the cause of surges of large magnitude on overhead and buried conductors due to direct strikes to the lines or by induction. The former is becoming the more severe case and the latter is becoming the more common case.

4.3.1 MV Distribution Line

Medium voltages usually include the voltages 1 kV → 36 kV[32]. When the lightning surges occurs on the MV phase conductors, if the overvoltage exceeds the breakdown strength of the line insulator string, the voltage waveforms is similar to the following in Fig 4.3 [36].

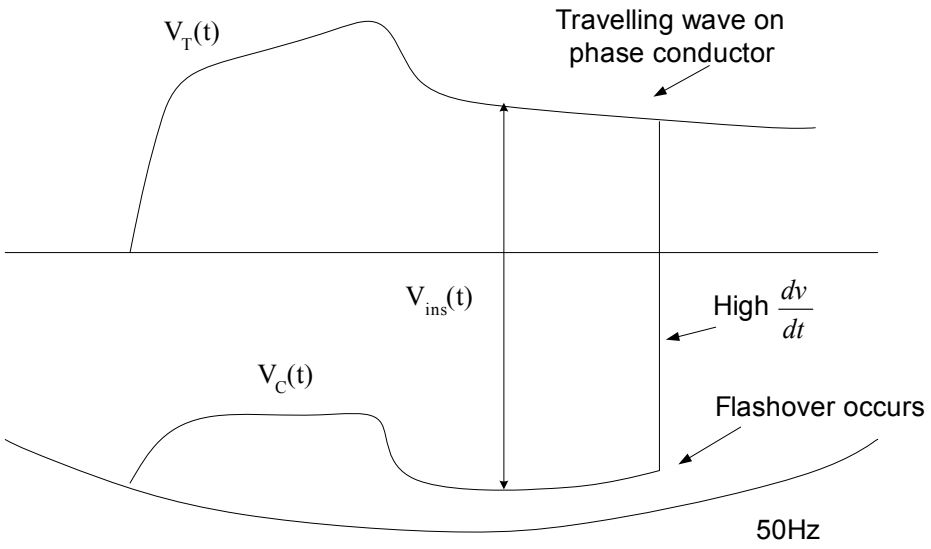

Fig 4.3 Lightning surge waveform on MV phase conductor

Where $V_T(t)$ is the voltage at the top of the pylon (we assume the crossarm coincides with the top of the pylon)

$Vc(t)$ is the voltage on the phase conductor(sum of the power frequency voltage and the coupled surge voltage)

$Vins(t)$ is the voltage across the insulator string (= $V_T(t)$ - $Vc(t)$)

Multiple pole flashover has beneficial consequences in that the larger the number of poles where flashover occurs.

- The lower the stresses on the network surge arresters(lightning current flows to earth through the poles rather than along the phase conductors towards surge arresters)

- The less the pole damage (reduced lightning current through individual poles)
  Uniform pole footing resistance is desirable for equal current sharing

Lowering the BIL of a line (installing an earth strap down wooden poles) limits the magnitude of surges propagating down the line towards line equipment (equivalent to installing spark gaps); however large amplitude surges are also induced in the line during adjacent lightning strikes. If the BIL of the line is too low there will be an unacceptably large number of line flashovers associated with induced surges.

4.3.2 MV/LV Transformer

For a MV/LV distribution transformer, it is not just the primary winding which is at risk, typically 50% of the lightning surge amplitude is transferred across the transformer unless there is a high capacitance cable on the secondary [36].

A transformer in general possesses a number of internal resonance which are governed by the winding construction. Larger transformers in general show lower resonance frequencies than smaller transformers. When overvoltage occurs on the transformer due

to lightning maximum values of oscillations are determined by the capacitances and inductances.

The hazard from separate earth electrodes is realized during high frequency current discharges by the MV surge arresters. During these times, the potential of the transformer tank is raised to the voltage drop across the MV earth lead inductance and the MV earth electrode impedance. High tank potentials stress the insulation between the LV windings and the transformer tank and core. Repeated insulation stress may lead to transformer failure.

A neutral surge arrester may suffer damage from overheating if a sustained voltage of magnitude greater than 5 KV is applied across its terminals. A damaged surge arrester may open or short circuit. In the latter case, high power frequency voltages may be transferred to the customer.

4.3.3 Domestic Consumer

If lightning strikes the lightning protection system of a building, and the earth impedance is low, most of the lightning current flows to earth. However, if the earth impedance is large, the voltage between the lightning protection system and the electrical system inside the building could be large enough to cause insulation flashover, SPD operation or damage to unprotected equipment.

SABS IEC 1312-1 (1995) proposes the possible distribution of the lightning current between the various paths as shown in Fig 4.4 [2].

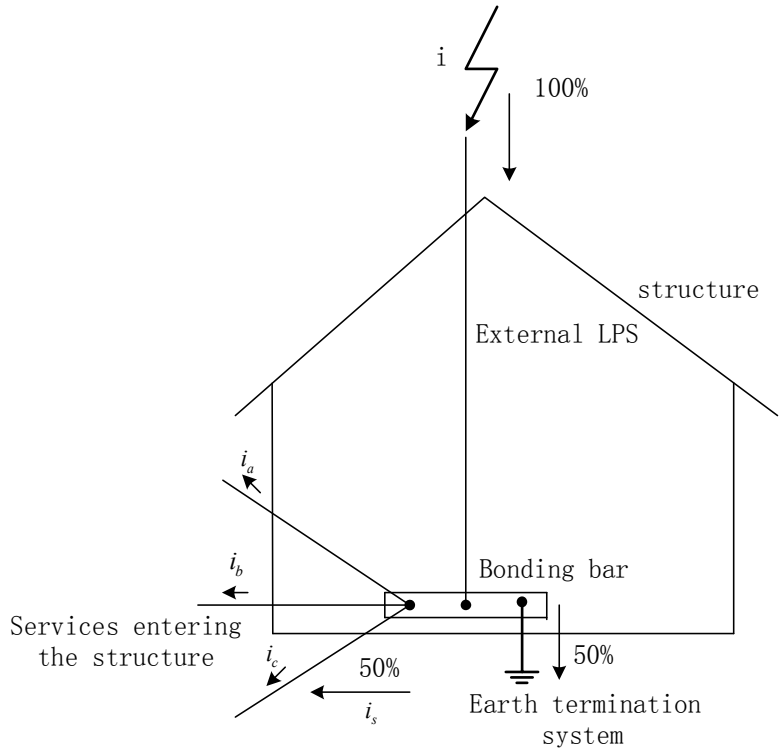

Fig 4.4 Lightning current distribution between the services to the structure

It can be assumed that where a total lightning current i strikes a building, 50% of i is distributed among the services entering the structure:

$$\begin{aligned} & i_a + i_b + i_c \quad (distributed\ in\ n\ services) \\ & = i_s = 0.5i \end{aligned} \tag{4.5}$$

i_s is assumed to be distributed equally among the services: for service x

$$i_x = \frac{i_s}{n} \tag{4.6}$$

If each service comprise m discrete conductors or cores, the current in each core, i_{cx} is

$$i_{cx} = \frac{i_s}{nm} \tag{4.7}$$

A telephone line shall be assumed to carry 5% of I, and shall not be included in n. In shielded cables the current i_x will flow along the shield. A small residual current will flow in the cores, and IEC 81(sec) 60 i proposes the following: $i_x x = i_s / n$ flows in the shield/cores combined. This is divided as 95% on the shield and 5% distributed amongst the m cores.

$$i_{cx(shield)} = 0.05\frac{i_s}{nm} \tag{4.8}$$

$$i_{x(shield)} = 0.95\frac{i_s}{n} \tag{4.9}$$

Nixon gives an example to show the lightning distributed current on a telephone core in terms of a protection level Ⅲ structure shown in Table 4.2, the result is that if the telephone line is not shielded, each core (two cores) will be subjected to 12.5 KA (10/350 μs), if the telephone line is shielded, each core will be subjected to 62.5 A only [32].

The flow of partial lightning current through conductors that form part of the earth electrode may result in coupling with nearby signal and power cables which may result in damaging transient overvoltages if adequate protection is not provided. This means that with the increasing sensitivity of electronic equipment (such as computers), significant interest has been raised in electromagnetic compatibility issues in lightning protection.

4.3.4 Touch, Step and Transferred Potentials

When surge currents enter metal objects on the surface of the earth, this could develop:

- Touch potentials at equipment, metal structures and metal fences in the vicinity of any electrical installation.

- Step potentials in the vicinity of any electrical installation, and particularly in the free spaces and operating positions in substation and high yards and outside boundary fences.

- Transferred potential of any conductive pipes, cables or other metal structures connected to some earthed point in the electrical installation but extending beyond the resistance volume of an earth electrode.

During an earth-fault, steel structures and all conducting metal parts that are bonded to the earth electrode will rise in potential to the same value as the total potential rise of the earthing system. A serious hazard can therefore arise during a fault, owing to the transfer of high potentials between a conductor or structure connected to the earth electrode or unbounded structure within the resistance volume of the earth electrode and other metalwork not bonded to the earth electrode of the substation but connected to a remote "earth".

When the potential lies in the vicinity of a vertical rod or a buried horizontal conductor the gradient between two points at distances S_1 and S_2 from the electrode [4]

$$U_{step} = \frac{\rho \cdot I}{2\pi}\left(\frac{1}{S_1} - \frac{1}{S_2}\right) \tag{4.10}$$

When the potential lies in the vicinity of and within a complex earth electrode, such as through a grid, an approximation of the maximum touch potential [4] is

$$U_{touch} = \frac{\rho \cdot I}{\pi \cdot L} \cdot \left(\frac{1}{2}\ln\frac{W^2}{16H \cdot d} + \ln\alpha\right) \tag{4.11}$$

Where ρ = resistivity of surface layer of soil, Ω m

H = depth of burial, m

d = diameter of conductor, m

W = conductor spacing, m

L = total length of buried conductor, m

A = a factor depending on size of squares of grid

This method is reasonably accurate when used for calculation of the touch potential for the centre of a regular grid. The current flow per unit length of conductor which flows from a grid electrode will vary, being higher at the sides than in the centre and higher still at the corners of the grid. In such cases, an irregularity factor K_i is given [4].

$$U_{touch} = \frac{K_m \cdot K_i \cdot \rho \cdot I}{L} \tag{4.12}$$

Where K_m is a coefficient that takes into account the effect of the number n, spacing W, diameter d and depth of burial H of the grid conductors,

$$K_m = \frac{1}{2\pi} \ln \frac{W^2}{16Hd} + \frac{1}{\pi} \ln\left(\frac{3}{4}\right)\left(\frac{5}{6}\right)\left(\frac{7}{8}\right) \text{ …….etc.} \tag{4.13}$$

K_i = an irregularity correction factor allowing for non-uniformity of current.

ρ = average resistivity of the ground, Ω m

L = total length of buried conductor, m

Measures to reduce touch and step potentials

- In positions where operators must handle equipment, provide an earth mat large enough for the operator to stand upon, and connect it to the operating handle and metalwork of the equipment. Using rubber mats, rubber gloves and rubber boots can reduce touch and step potentials of operating personnel.

- If a rod is driven from the bottom of a pit or trench, a horizontal conductor is buried deeper into the earth. By insulating the earth lead to the rod electrode, the surface potential gradients are reduced.

4.4 The Effect of Soil Resistivity on Surge Generation

On transmission lines, the lightning performance, especially with regard to the back-flashover mechanism, is largely determined by the impedance of the pole footing at the time of peak current.

An MV distribution line phase conductor subjected to a lightning strike is shown in Fig 4.5.

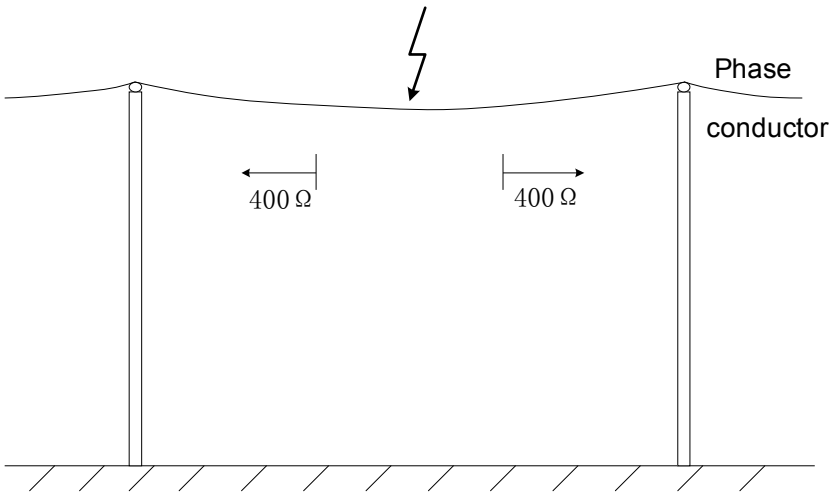

Fig 4.5 Lightning strike to a MV phase conductor

The surge impedance of a typical MV phase conductor is approximately 400 Ω and thus the impedance seen by the lightning surge (modeled as a current source) is 200Ω (given by 400Ω ‖ 400Ω as the current travels in both directions). If the line BIL is 300KV, the minimum value of lightning current necessary to cause flashover is therefore

$$I_{crit} = \frac{BIT}{Z} = \frac{300kV}{200\Omega} = 1.5kA \quad (4.14)$$

Virtually all lightning currents exceed this value and hence flashover occurs with almost every direct strike. Once flashover has occurred, the lightning then sees a high pole footing resistance due to the relatively high soil resistivity and hence the phase conductor remains at a high voltage with respect to a remote earth [35].

Direct strikes usually result in flashover and hence can give rise to common mode surges of up to several megavolts. The overvoltage waveform resulting from flashover is generally referred to as a chopped waveform. The rise-time follows that of the current waveform until flashover occurs, at which instance the voltage then drop to zero.

4.4.1 Lightning Electromagnetic Fields Generated by Lightning Return Stroke

4.4.1.1 Vertical Electric and Azimuthal Magnetic Field

Due to technical difficulties associated with measuring the characteristics of lightning, many researchers have resorted to numerical models to derive the features of lightning electromagnetic fields generated by lightning return strokes

For the vertical component of the electric field and the azimuthal magnetic field, at distances from the lightning channel not exceeding a kilometer, their intensity can be calculated with reasonable approximation assuming that the ground is as a perfect conductor. Making reference to Fig 4.6, expressions for the total vertical electric and azimuthal magnetic field in the frequency domain are given [47] as:

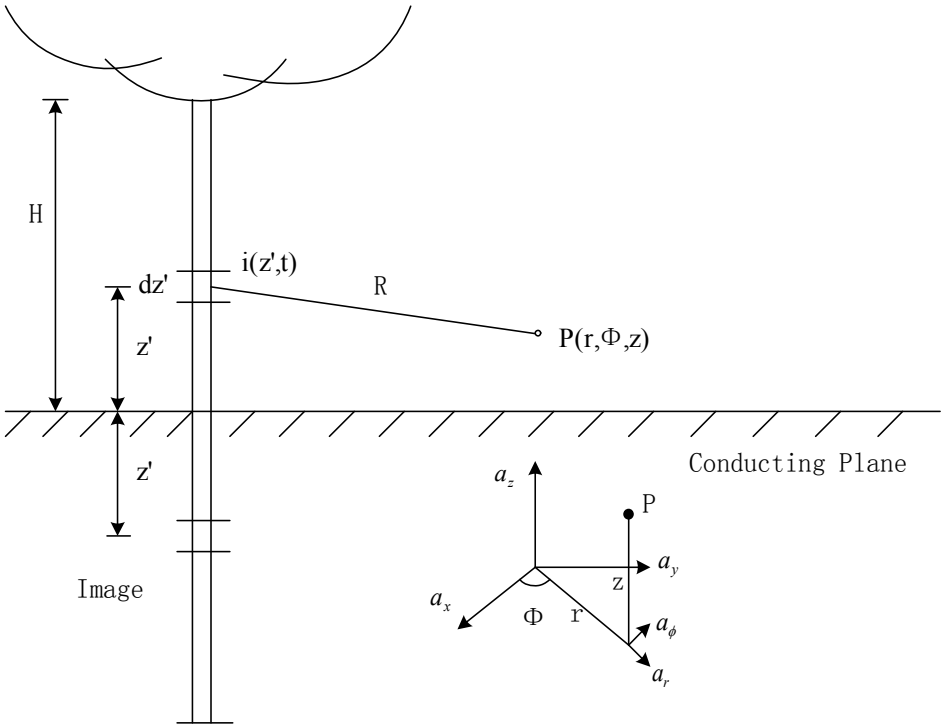

Fig 4.6 Geometry for the calculation of lightning return-stroke electromagnetic fields

$$E_z(r,z,j\omega)=\frac{1}{4\pi\varepsilon_0}\left[\int_{-H}^{H}\frac{2(z-z')^2-r^2}{R^5}\frac{1}{j\omega}I(z',j\omega)\cdot\exp(-j\omega R/c)dz'\right.$$
$$+\int_{-H}^{H}\frac{2(z-z')^2-r^2}{cR^4}I(z',j\omega)\cdot\exp(-j\omega R/c)dz' \qquad (4.15)$$
$$\left.-\int_{-H}^{H}\frac{r^2}{c^2R^3}j\omega I(z',j\omega)\cdot\exp(-j\omega R/c)dz'\right]$$

$$H_\Phi(r,z,j\omega)=\frac{1}{4\pi}\left[\int_{-H}^{H}\frac{r}{R^3}I(z',j\omega)\cdot\exp(-j\omega R/c)dz'\right.$$
$$\left.+\int_{-H}^{H}\frac{r}{cR^2}j\omega I(z',j\omega)\cdot\exp(-j\omega R/c)dz'\right] \qquad (4.16)$$

Where r is horizontal distance between lightning channel and observation point

z is height of a dipole with respect to ground's surface

H is lightning-channel height

c is speed of light in free space

ε_0 is permittivity of free space

$I\left(z^{'}, j\omega\right)$ is the Fourier transform of the current distribution along the lightning channel $i\left(z^{'}, t\right)$, determined using a given lightning return stroke current model, and,

$$R = \sqrt{r^2 + \left(z - z^{'}\right)^2} \tag{4.17}$$

For distance ranges beyond several kilometers, the propagation over a ground of finite conductivity results in a noticeable attenuation of high frequency components of the fields. However, for these range of distances, the inducing effect of lightning becomes less important.

The assumption of a perfect conducting ground allows us to obtain closed-form expressions for the fields in the time domain. These are:

$$\begin{aligned} E_z\left(r, zt\right) = \frac{1}{4\pi\varepsilon_0}\Bigg[& \int_{-H}^{H} \frac{2\left(z - z^{'}\right)^2 - r^2}{R^5} \int_0^t i\left(z^{'}, \tau - R/c\right) d\tau \, dz^{'} \\ & + \int_{-H}^{H} \frac{2\left(z - z^{'}\right)^2 - r^2}{cR^4} i\left(z^{'}, t - R/c\right) dz^{'} \\ & - \int_{-H}^{H} \frac{r\left(z - z^{'}\right)}{c^2 R^3} \frac{\partial i\left(z^{'}, t - R/c\right)}{\partial t} dz^{'} \Bigg] \end{aligned} \tag{4.18}$$

$$\begin{aligned} H_{\Phi}\left(r, z, t\right) = \frac{1}{4\pi}\Bigg[& \int_{-H}^{H} \frac{r}{R^3} i\left(z^{'}, t - R/c\right) dz^{'} \\ & + \int_{-H}^{H} \frac{r}{cR^2} \frac{\partial i\left(z^{'}, t - R/c\right)}{\partial t} dz^{'} \Bigg] \end{aligned} \tag{4.19}$$

4.4.1.2 Ground Effects on the Horizontal Electric Field Component

The horizontal component of the electric field radiated by lightning is more effected by the ground finite conductivity. Although at some meters above ground its intensity is much smaller than that of the vertical component.

In this section we will consider and compare the following simple approximations

- Wavetilt Formula

  The wavetilt formula [50] expresses the ratio of the Fourier transform of the horizontal electric field $E_r(j\omega)$ to that of the vertical field $E_z(j\omega)$ and thus, allows calculating the horizontal component of the electric field over a soil of finite conductivity from the knowledge of the vertical component of the same field. The wavetilt formula is shown below:

$$W(j\omega) = \frac{E_r(j\omega)}{E_z(j\omega)} = \frac{1}{\sqrt{\varepsilon_{rg} + \dfrac{\sigma_g}{j\omega\varepsilon_0}}} \tag{4.20}$$

  Where σ_g , ε_{rg} are the ground conductivity (inverse of soil resistivity) and relative permittivity, respectively.

  The use of this function for the case of lightning is reasonable only for far observation points; its application for close distances may describe only the first microseconds of the horizontal field.

- Cooray Approach

  Cooray [51] proposed to calculate the horizontal electric field at the surface of a finitely conducting ground making use of the expression for the surface impedance of the ground. The horizontal electric field at ground level can be determined from the azimuthal magnetic field using the surface impedance expression, as follows

$$E_r(r,0,j\omega) = B_\phi(r,0,j\omega)\frac{c}{\sqrt{\varepsilon_0\varepsilon_{rg} + \sigma_g / j\omega\varepsilon_0}} \qquad (4.21)$$

Where $E_r(r,0,j\omega)$ and $B_\phi(r,0,j\omega)$ are the Fourier-transforms of the horizontal electrical electric field and of the azimuthal magnetic induction at ground level respectively.

Cooray has also shown that the simplified formula yield very accurate results at distances as close as 200m from the lighting channel.

- Rubinstein Approach

  Rubinstein [52] has proposed a new approach according to which the horizontal electric field can be viewed as decomposed into two terms: the first one is the horizontal field calculated assuming the ground to be perfectly conducing. The second one is a correction factor given by the product of the magnetic field, calculated assuming the ground to be a perfect conductor, and a function similar to the wavetilt one, which represents the effect of the finite ground conductivity. The horizontal electric field at a distance r and at a height z over the ground is given by:

$$E_r(r,z,j\omega) = E_{rp}(r,z,j\omega) - H_{\phi p}(r,z,j\omega)\frac{1+j}{\sigma_g\delta_g} \qquad (4.22)$$

Where $E_r(r,z,j\omega)$ and $H_{\phi p}(r,z,j\omega)$ are the Fourier-transforms of the horizontal component of the electric field at height z, and of the azimuthal component of the magnetic field at ground level respectively. Both are calculated assuming a perfect conducting ground, and δ_g is the skin-depth in the ground.

The basic assumption is that $\sigma_g \gg \omega\varepsilon_0{\varepsilon_{rg}}^2$. (4.22) can be written in the following more general form

$$E_r(r,z,j\omega) = E_{rp}(r,z,j\omega) - H_{\phi p}(r,z,j\omega)\frac{c\mu_0}{\sqrt{\varepsilon_{rg} + \sigma_g / j\omega\varepsilon_0}} \quad (4.23)$$

Since that the second term in (4.23) is identical to the formula proposed by Cooray for the calculation of the horizontal electric field at ground level, we will call equation (4.23) the Cooray-Rubinstein formula.

A systematic application [53] of the approximate expressions for calculating the return stroke horizontal electric fields has been performed for the different ground conductivities and distances, namely 200 m, 500 m, 1.5 km, assuming a ground conductivity of $10^{-2} S/m$ and a relative ground permittivity of 10. The calculated results were compared with the very accurate and mathematically more complex approximations. The comparison shows that:

- At very close distance range (r = 100 – 200 m), and for ground conductivities of about $10^{-2} S/m$ or higher, the perfect conducting ground assumption can be considered as reasonable for an observation point located at a few meters above ground.

- The Cooray-Rubinstein formula permits to obtain satisfactory results for all the considered ranges. It is the only one that reproduces satisfactorily the bipolar waveshape of the horizontal electric field at intermediate distance ranges.

The vertical electric field, not affected significantly by the ground conductivity, is shown only for the perfectly conducting ground. However, the horizontal electric field is greatly affected by the ground conductivity, and can be calculated in an accurate way using the Cooray-Rubinstein simplified formula.

4.4.2 High Frequency Characteristics of Impedances to Ground

Takashima [27] described the high frequency characteristics of impedances to ground by the current simulation method together with the method of images.

When high frequency current is injected into a ground electrode and the conductivity of the earth around the electrode is low (the soil resistivity is high), the impedance rather than the dc resistance needs to be used as the circuit element from the electrode to the earth, in the circuit consideration. High frequency characteristics of the impedances to the earth as well as the field distributions of some typical electrodes are calculated by the current simulation method together with the method of images.

As the frequency of injected current increases, the potentials and field intensities on the earth's surface in the vicinity of the electrode decrease in a similar degree independently of the distance from the electrode, as the frequency increases, the potentials and intensities decrease more than the impedance decreases.

The lightning waveform can be closely approximated by the (double-exponential) equation:

$$I(t) = I_0\left[e^{-\alpha t} - e^{-\beta t}\right] \tag{4.24}$$

where: I_0 ,α, β are parameters dependent on the actual waveform

The formula can be expressed in the frequency domain by applying the Fourier transform:

$$F(\omega) = \int_{-\infty}^{+\infty} f(t) e^{j\omega t} dt = I_0\left(\frac{1}{\alpha + j\beta} - \frac{1}{\beta + j\omega}\right) \tag{4.25}$$

Two standard types of waveforms have been defined by IEC 61000-4-5: 1.2/50 μs and 8/20 μs .

4.4.3 Lightning Strikes to a Building

When designing a lightning protection scheme for a building, several scenarios must be considered: directly to the building, directly to overhead low-voltage distribution lines outside of the building directly, to other objects near the building, distant cloud-to-earth strokes, and cloud-to-cloud discharges. The two most severe cases of lightning termination must be examined: a direct stroke to one building and to overhead low-voltage distribution lines outside of the building.

For a low-voltage power distribution system, different countries have adopted different practices on earthing the neutral conductor, two approaches are well entrenched in their respective territories, the so-called TN system and TT system where the difference lies in the mode of earthing the neutral. For TT system the neutral is earthed only at the distribution transformer secondary, and the protective earth in a building is obtained from a local earth electrode, the TN system has its neutral earthed at any available opportunity outside of a building, including the distribution transformer secondary, some or all poles, and the service entrance.

Mansoor [37] postulated some events to model the distribution system. One of the events is shown in Fig 4.7, which shows a schematic of a 2-phase 3 wire TN 120/240V service to a building.

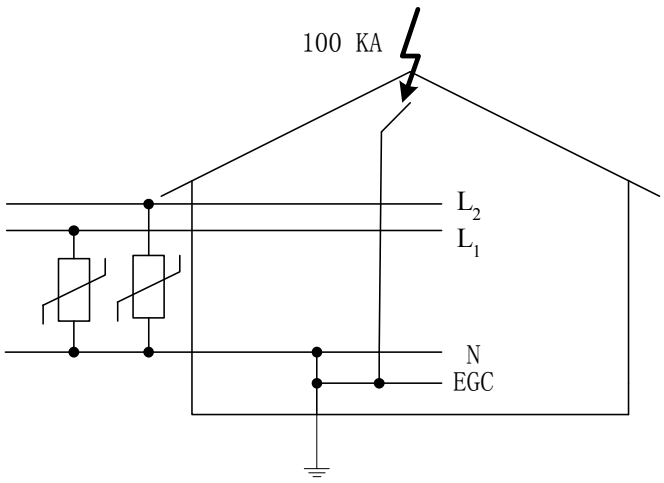

Fig 4.7 Service connections in a 3-wire TN system

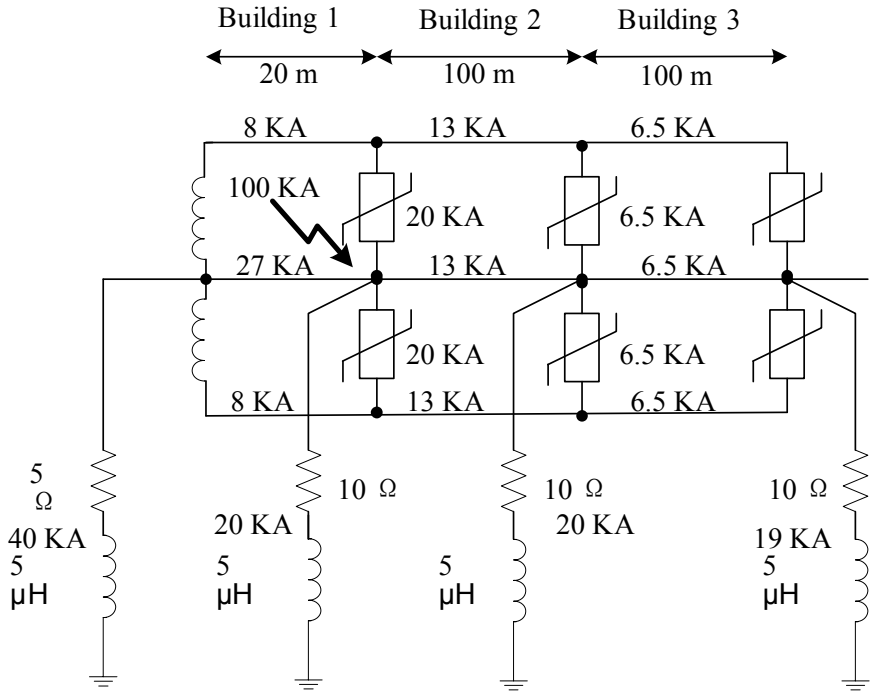

Fig 4.8 TN configuration with building next to the transformer struck by a 10/350 μs, 100 kA surge, showing peak currents.

When a distribution transformer supplies three buildings along a street, with short service drops from the poles to each building, the lightning strike is postulated to occur upon the first building, next to the transformer. The peak current distribution in each branch is shown in Fig 4.8 according to the measurement values, and the waveforms of currents leaving building are shown in Fig 4.9.

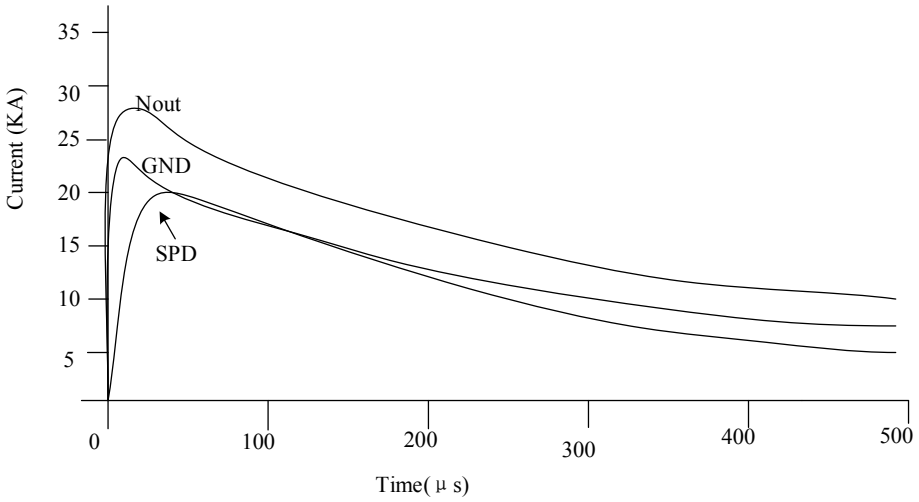

SPD – Current into each line of service drop, through SPDs

GND – Current into local building earth electrode

Nout – Current into neutral conductor toward the transformer earth

Fig 4.9 Waveforms of currents leaving building 1, as defined in Fig 4.8, for a 100 kA, 10/350 μ s surge terminating on the building earthing system.

If the lightning strike is postulated to occur upon the third building the peak current distributions in each building earth electrode from transformer to the third building are 40kA, 19kA, 25kA and 42kA. Mansoor compared the results from the two cases and found that the greater the distance of a building, which subjected to a lightning surge, from the transformer earth electrode, the more the current flow in the building earth. He also found that the earthing connection of a building did not carry anywhere near the 50% peak current.

Mansoor postulated a 5-Ω pole earthing resistance and a 10-Ω building earthing resistance. Table 4.3 shows the comparison of the baseline case with the reversed relationship between the pole earthing resistance and the building earthing resistance.

Table 4.3 Effect of pole earthing/building earthing – TN radial

Percent of 100 KA peak	Baseline 5-Ω pole,10-Ω building	Reverse baseline 5-Ω building,10-Ω pole
Current in building earth	21	31
Current in service earth	33	14
Current in SPD	23	22

From the Table 4.3 the relationship of pole versus building earthing resistance has a significant effect on the current carried by the neutral, but not on the current carried by the SPDs.

4.5 Summary

The types of surges and the effect of surges on power networks have been discussed. The lightning surges have been highlighted. The effect of ground conductivity on lightning electromagnetic fields has been discussed as well.

Surges are caused in distribution systems by internal overvoltages and external overvoltages. Switching surges usually occur together with 50 Hz power frequency overvoltages. Lightning and temporary overvoltages are the major influencing factors in distribution networks.

A lightning strike from a cloud to ground has a significant effect on the LV power networks. Fortunately this accounts for about 10 percent of lightning discharges only. Direct strikes have higher peak current and voltage magnitudes than indirect strikes; therefore direct strikes are often the cause of severe damage to power systems. In a lightning strike, once the flashover occurs on the transmission line, the lightning then sees the high pole footing resistance due to the relatively high soil resistivity. The transmission line BIL is designed to limit the number of flashovers due to indirect strikes.

When calculating the return stroke horizontal electric fields, at very close distance (less than 200 m) from the lightning channel and for ground conductivities of about $10^{-2} S/m$ or higher, the perfect conducting ground assumption can be considered as reasonable for an observation point located at a few meters above ground.

The vertical electric field, not affected significantly by the ground conductivity, is shown only for the perfectly conducting ground. However, the horizontal electric field is greatly affected by the ground conductivity, and can be calculated in an accurate way using the Cooray-Rubinstein simplified formula.

If earth impedance is low, most of the lightning current that strikes the lightning protection system of a building can flow to earth. This would reduce the damage to domestic appliances. Soil resistivity also has a direct influence on touch potentials and step potentials.

Chapter 5

SURGE PROPAGATION

This chapter introduces the process of surge propagation and the factors affecting it. Distribution transformer models and transfer functions are used to describe the effect of transformers on surge propagation. It also presents the model of transmission lines and footing resistances used to show the effect of soil resistivity. A theoretical analysis and formulation on the influence of ground conductivity on lighting-induced voltages on an overhead wire are presented. The functions and effects of SPDs on surge propagation are discussed.

5.1 Propagation of Lightning Surges

Lightning surges are transferred from the MV to the LV side of distribution transformers. This involves accurate simulation of the transfer of surges from MV to LV networks and the subsequent propagation of the modified waveform along the LV distributor.

5.1.1 MV Surges

If lightning strikes a medium voltage distribution network, large overvoltage surges occur. These overvoltages are seen by the primary side of the distribution transformer that steps the MV down to LV to be delivered to consumers.

The distribution transformers have a BIL of 150kV for 22kV equipment, hence transformers require protection on the MV side as the basic insulation level of a 22 kV line is typically 300 kV or more, this involves the installation of surge arresters to clamp any surge voltages which could damage the transformer insulation [35].

5.1.2 The Effect of the Transformer

The distribution transformer is not an ideal linear system. It possesses certain non-linearity, the degree of which varies for different frequency ranges. In order to make use of the concept of the transfer function for the modeling of the distribution transformer, it must be assumed that the transformer behaves linearly or approximately linearly under the conditions in which the transformer will be simulated.

Numerous papers have been published on the modeling and behavior of power transformers under transient conditions. This section summarizes research done on transformer modeling and transfer functions under lightning surge conditions.

5.1.2.1 Transformer Model

In the propagation of transients through transformers, two main transfer functions are used: the propagation transfer function and the characteristic admittance. It is useful to choose the right accuracy for their rational approximation.

Kelly [41] presented a high frequency transformer model. The basic idea is to produce an equivalent network whose nodal admittance matrix matches the nodal admittance matrix of the original transformer over the frequency range of interest. Such representation would correctly reproduce the transient response of the transformer at its terminals. The model is thus ideally suitable for the calculation of transients involving the interaction between the system and the transformer.

The relation between the voltage and currents at the accessible terminals of a transformer can be expressed using the nodal matrices:

$$[Y][V] = [I] \tag{5.1}$$

For a three phase system, equation (5.1) can be expressed as:

$$\begin{bmatrix} Y_{11} & Y_{12} & \cdots & Y_{1m} \\ Y_{21} & Y_{22} & \cdots & Y_{2m} \\ \vdots & \vdots & & \vdots \\ Y_{m1} & Y_{m2} & \cdots & Y_{mm} \end{bmatrix} \begin{bmatrix} V_1 \\ V_2 \\ \vdots \\ V_m \end{bmatrix} = \begin{bmatrix} I_1 \\ I_2 \\ \vdots \\ I_m \end{bmatrix} \tag{5.2}$$

$$[Y_{ij}] = \begin{bmatrix} y_{ij,aa} & y_{ij,ab} & y_{ij,ac} \\ y_{ij,ba} & y_{ij,bb} & y_{ij,bc} \\ y_{ij,ca} & y_{ij,cb} & y_{ij,cc} \end{bmatrix} \tag{5.3}$$

Where $[Y_{ij}]$ is 3×3 sub-matrix and m is the number of three-phase terminals under consideration. Thus for a Delta-Wye, three phase transformer, Fig 5.1 shows a single line diagram of the multi-terminal π-equivalent network. For simplicity, only one-phase terminals from each of the primary and secondary winding are shown.

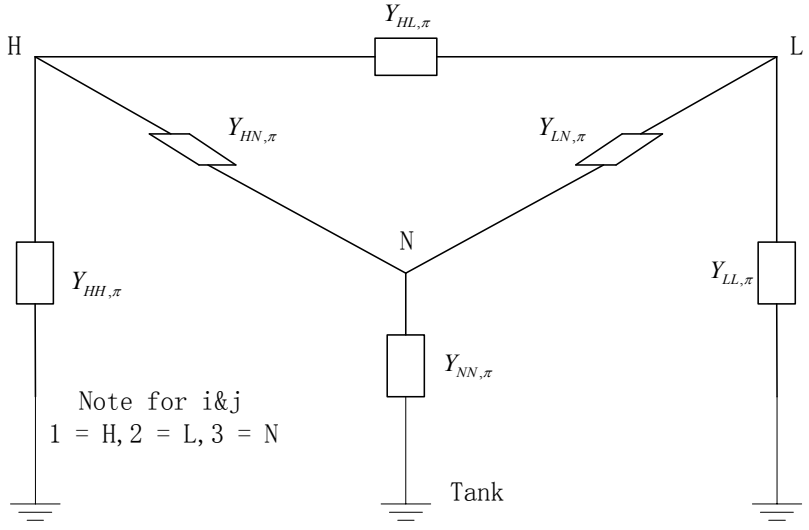

Fig 5.1 Single-line diagram of the multi-terminal π-equivalent

A typical RLC module used in the approximation of the elements of $[Y_{ij}]$ is shown in Fig 5.2. These RLC networks reflect the known frequency characteristics of the admittance functions of the transformer:

- Inductive behavior at low frequencies.
- Series and parallel resonances of mid to high frequencies.
- Predominantly capacitive behavior at high frequencies.

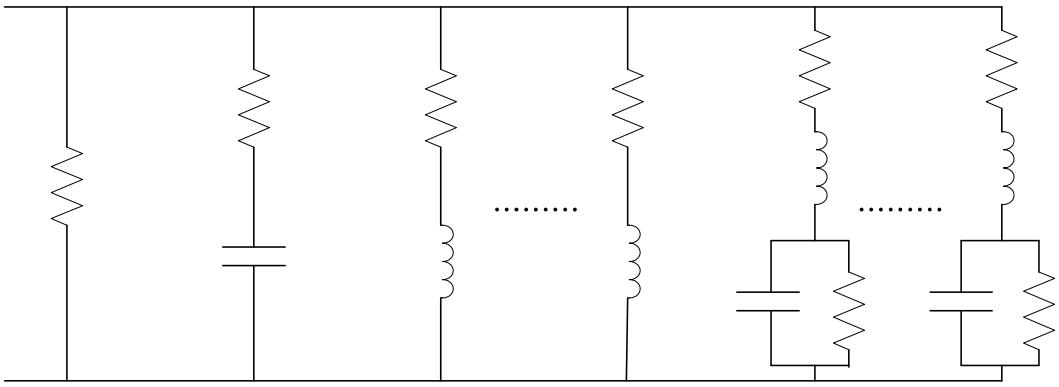

Fig 5.2 Structure of an RLC module

When the related parameters of the above RLC branch are given, the three terminal π - equivalent model can be described, and the transient response of the transformer could be calculated.

Lightning surges propagating through the system may excite the transformer at its resonant frequencies. The frequency spectrums of typical lightning waveforms contain high frequency components that can extend into the megahertz range.

5.1.2.2 Transfer Function

One of the dielectric tests performed by Hanique[14] on a transformer is the lightning impulse test. The transfer function is an additional tool to determine if a transformer passed the lightning impulse test. In theory the transfer function is independent of the waveshape of the time-domain signal.

P.T.M. Vaessen [28] proposed a method of system characterization by the analysis of its frequency behavior that is called frequency response analysis (FRA) and is gradually being introduced in the field of power transformer testing and diagnosing. The proposed FRA technique is in use as a diagnostic tool in addition to the lightning impulse testing of transformers.

The two port model of a single phase transformer in Fig 5.3 can be described according to network theory with the hybrid parameters Y_{1n}, H_{12} and Z_{2s}:

$$I_1 = Y_{1n}V_1 - H_{12}I_2 \tag{5.4}$$

$$V_2 = H_{12}V_1 + Z_{2s}I_2 \tag{5.5}$$

Where Y_{1n} is the primary no-load admittance, H_{12} is the no-load voltage transfer from primary to the secondary side and Z_{2s} is the secondary short-circuit impedance. Essential in this network description are the assumptions of linearity and reciprocity of the transformer.

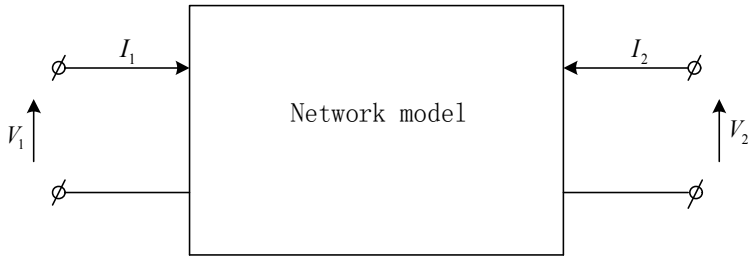

Fig 5.3 Two-port network model for a single-phase transformer

In order to verify the validity of the assumptions of linearity and reciprocity the primary short-circuits admittance of a 25 MVA 150/11 KV transformer [28] was measured directly and calculated from the measured hybrid parameters according to:

$$Y_{1s} = Y_{1n} + H_{12}^{\ 2} / Z_{2s} \qquad (5.6)$$

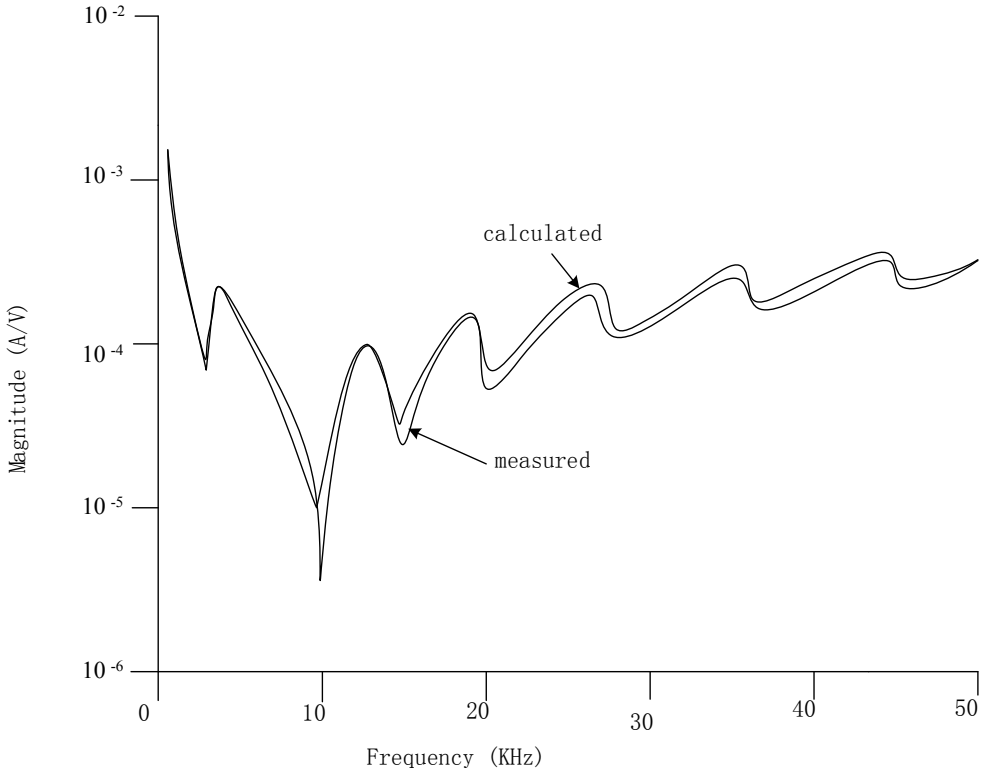

Fig 5.4 Measured and calculated primary short-circuit admittance for a 25 MVA 150/11 kV transformer

The results are shown in Fig 5.4. The voltage transfer function of a l MVA 10/0.4 KV distribution transformer was also calculated from measurements performed in a compact test setup with both low voltage (250 V) and high voltage (25 KV) lightning impulses to verify the linear behavior. These results are presented in Fig 5.5. From these two types of results the conclusion must be that the transformer behaves linearly enough to justify the systems approach.

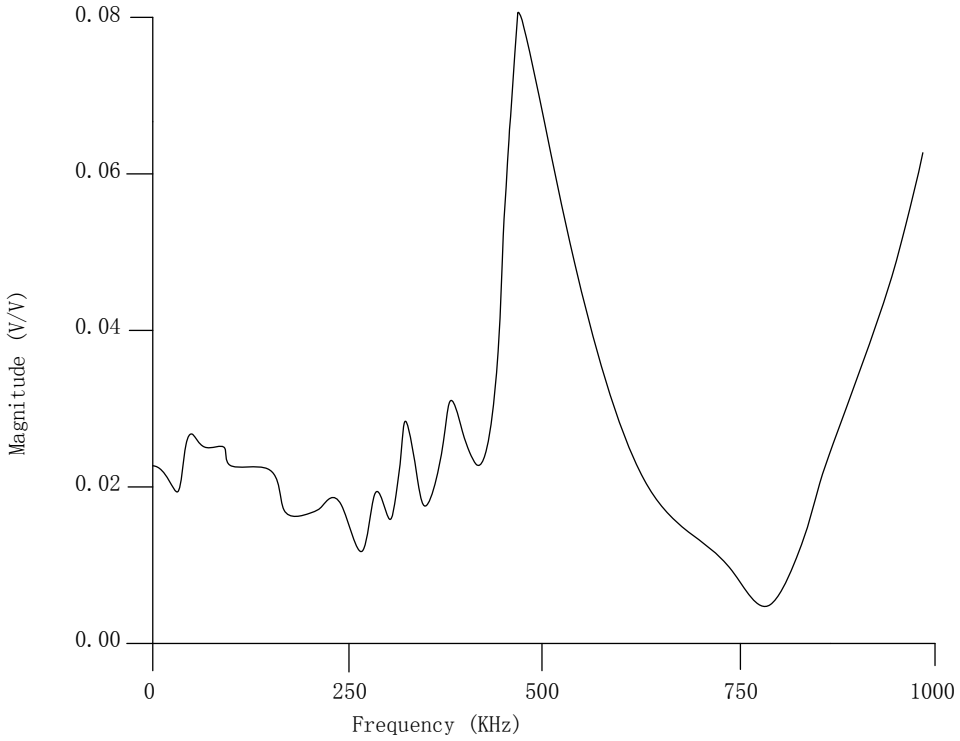

Fig 5.5 Calculated voltage transfer of a 1MVA 10/0.4 kV transformer for different test voltages

5.1.3 The Effect of Earthing on Surge Propagation

In order to provide MV surge arresters with a discharge path for surge currents, an earth electrode should be supplied on the MV side. The voltage developed across a surge arrester during surge current discharge is limited but the voltage developed across the earthing lead inductance and earth electrode impedance may be large. The combined voltage across the arrester and earthing system may be sufficient to cause breakdown of the insulation between the MV phases and transformer tank or core. By connecting the surge arrester directly to the tank, and connecting the tank to earth, the voltage stress across the insulation is limited to the arrester discharge voltage. During surge discharges,

the potential of the transformer tank is raised to the voltage drop across the earthing system.

A surge arrester is connected between the MV neutral (to which the transformer tank is bonded) and the LV neutral to limit the voltage stress across the LV winding-to-core insulation during MV arrester discharges.

The reasons for earthing the neutral of an LV system [6] are:

- To provide a conductive return path for any earth fault and earth leakage current;
- To maintain the neutral of the LV system as close as possible to earth potential;
- To ensure that the MV protection operates in the event of a fault between the MV and LV windings of a transformer; and
- To reduce the prospective touch voltage as much as is reasonably practical.

5.1.4 The Factors Affecting the Transient Behavior of Earth Electrodes

The principle factors that affect the transient behavior of an earth electrode are summarized as being:

- Geometry and arrangement of the earth electrode
- Dielectric nature of the soil
- Non-linear time-varying effects of soil ionization
- Electromagnetic interaction with adjacent conductors

The geometry and configuration of an electrode determine the amount of conductor surface area in contact with the soil and therefore affect the resistance of the earth electrode. Furthermore, a longer electrode will have a larger self-inductance which will increase the surge impedance of the earth electrode. It is therefore essential to include the effect of geometry in modeling [31].

At higher frequencies, the dielectric nature of soil decreases the impedance of the earth electrode, but the resulting decrease is less than 15% for typical lightning frequencies and soil condition [30].

It is well established that the lightning transient performance of an earth electrode differs from the performance under a power frequency fault.

The impulse impedance of electrodes can differ significantly from their low-voltage power-frequency resistance values. This is due to one or more of the following phenomena:

- The self-inductance of the electrode.
- The frequency-dependent dielectric properties of the soil.
- Ionization and discharge processes in the soil.

The self-inductance of an electrode only contributes significantly to its impulse response when very high frequencies are involved or where the overall dimensions of the electrodes are very large. For a typical lightning current waveshape, since the dimensions of the electrodes are less than approximately 20m in most transmission line tower earthing arrangements, this study is, therefore, limited to the effect of ionization and the frequency-dependent dielectric properties of soil on the lightning impulse response of practical electrodes.

5.2 The Effect of Soil Resistivity on Surges

5.2.1 Footing Resistance

The two most important parameters which influence the lightning performance of transmission lines and which are controllable by the line designer are the insulation strength and the tower footing impedance. The impulse impedance of the tower footing, however, is an extremely difficult parameter to measure or estimate. The decrease in the impedance results from soil ionization under high-voltage conditions. Breakdown strength of soil, even in uniform electric fields, is a difficult parameter to measure. It is not only greatly influenced by the soil density, non-homogeneities and air gaps, but is also associated with long statistical delay times.

When a buried element of an earth electrode is subjected to a transient voltage such as that resulting from a steep-fronted lightning impulse current, it acts as a transmission line and various reflections must take place before the steady-state condition of low-frequency leakage resistance is reached.

The initial response of the electrode is termed the surge impedance and, as in the case of a transmission line, this depends upon the geometry of the buried electrode system and the soil resistivity.

In 1958, Korsuncev [44] applied similarity analysis to the surge response of ionized soil around footings. Footing resistances of differing ground electrode geometries can be represented by two dimensionless parameters,

$$\prod_1 = \frac{sR_i}{\rho} \tag{5.7}$$

$$\prod_2 = \frac{\rho I}{E_0 s^2} \tag{5.8}$$

Where s is a characteristic distance from the center to the outermost point of the electrode, m

ρ is the earth resistivity, Ω m.

E_0 is a critical breakdown gradient, 300 to 1500 kV/m.

I is the instantaneous value of current, kA.

R_i is the footing resistance, Ω

Oettle [30] showed that $\prod_1$ could be interpreted as a "normalized" impedance or as the impedance per unit resistivity for a unit length of electrode, and $\prod_2$ could be interpreted as the ratio between the theoretical electric field intensity at the surface of the electrode, $\left(\rho I / s^2\right)$ and the critical soil ionization constant E_0. Oettle stated that R_i was not only a function of the current, but also depended very much on the time at which it is calculated.

For each electrode geometry, defining a value of $\prod_1$ in terms of its low-frequency, low-current resistance, the resistance of a single driven rod in an infinite half-plane, in terms of rod length s, radius r and resistivity ρ is given by Rudenberg [46] as:

$$R_{rod} = \frac{\rho}{2\pi s} \ln\left(\frac{2s}{r}\right) \tag{5.9}$$

And thus, for the s/r ratio between 75 and 300:

$$\prod_1 (rod) = \frac{1}{2\pi} \ln\left(\frac{2s}{r}\right) = 0.8 - 1.0 \tag{5.10}$$

When Equation (5.10) is expressed in terms of characteristic distance s and surface area A = 2 π rs for a single driven rod, the following value of $\prod_1$ results:

$$\prod_1 (rod) = \frac{1}{2\pi} \ln\left(\frac{4\pi s^2}{A}\right) = 0.4028 + \frac{1}{2\pi} \ln\left(\frac{s^2}{A}\right) \tag{5.11}$$

In the case of the hemisphere, $A = 2\pi s^2$ so the ratio s^2 / A is a constant. Putting this into the same form as Equation (5.11) gives:

$$\begin{aligned} \prod_1 (hemisphere) &= \frac{1}{2\pi} = \frac{1}{2\pi} \ln(e) = \frac{1}{2\pi}\left(\frac{2\pi s^2 e}{A}\right) \\ &= 0.4517 + \frac{1}{2\pi} \ln\left(\frac{s^2}{A}\right) \end{aligned} \tag{5.12}$$

When Equation (5.12) is used for the ground rod, the error in estimating $\prod_1^0$ will be (0.4517-0.4028) = 0.0489, or about 6%. The Equation (5.12) can be used as a design tool for establishing footing geometries. Once ionized beyond the critical distance, all electrodes behave much like a hemisphere.

Several researchers have done experimental studies on the impulse response of ground electrodes. Fig 5.6 shows Liew and Korsuncev's [43] predicted "impulse resistance" versus current peak calculations for single-rod, two-rod and four-rod configurations.

Fig 5.6 shows that the initial resistance of the single rod is slightly lower with the new model, and the surge-reduced values fall more quickly with applied current. Both models converge to the same impulse resistance at high currents.

With the combination of ionization and surge-response model, the footing voltage V_f depends on the footing current I_f as follows:

$$V_f = 0.263 E_0 s \left(\frac{\rho I_f}{E_0 s^2}\right)^{0.692} \tag{5.13}$$

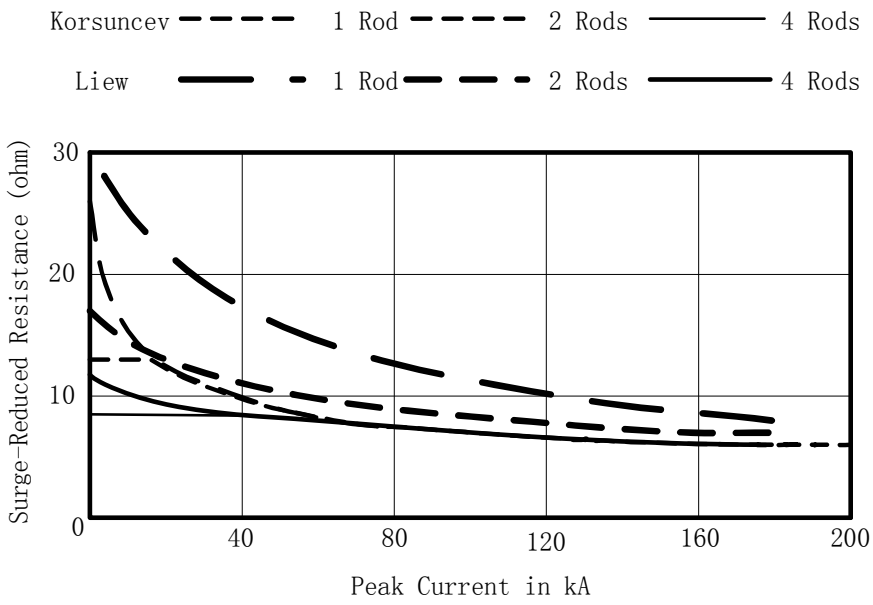

Fig 5.6 Surge-reduced footing resistance versus surge current for three electrode geometries

The footing resistance R_i as a function of footing current I_f [12]:

$$R_i = \frac{V_f}{I_f} = 0.263 E_0 s \left(\frac{\rho}{E_0 s^2} \right)^{0.692} I_f^{-0.308} \tag{5.14}$$

A comparison of predicted and observed outage rates for a transmission line geometry studied by Whitehead showed that when the ionization model alone is used, the predictions are too low, while when both ionization and footing surge response are induced, the overall curve matches the data better at both low and high footing resistances [12].

The Korsuncev criteria curve approach is attractive for calculation of footing resistance under lightning surge conditions. An extension of the model is introduced for calculation

of low-current footing resistance. The new model, based only on surface area and characteristic distance, applies for a wide range of ground electrode shapes.

To show the sensitivity of the surge-reduced footing resistance to the soil breakdown voltage Oettle [19] suggested a power-law regression between soil resistivity ρ and E_0 for a median value of breakdown gradient, giving

$$E_0 = 241\rho^{0.215} \tag{5.15}$$

When E_0 is 300kV/m, $\rho =$ 2.77 Ω m, then from Fig 5.6 and Equation 5.14 S can be derived.

5.2.2 The Propagation of Lightning Surges

Carlos T. Mata [21] did a triggered-lightning experiment shown in Fig 5.7. The facility included a test power line supported by fifteen poles. The line had two vertically stacked conductors, the top conductor being referred to as the phase conductor and the bottom conductor as the neutral. A total of four 10 kV distribution arresters were installed on the line, at pole 1,9,10, and 15, between the phase and the neutral conductors, and the neutral of the line was grounded at these four poles. Grounding of the lines neutral at these four poles was accomplished by means of 24 m copper vertically driven rods. The line was approximately 740 m long. The lightning current was directed to the phase conductor of the line between poles 9 and 10. During this particular event the arrester at pole 10 failed.

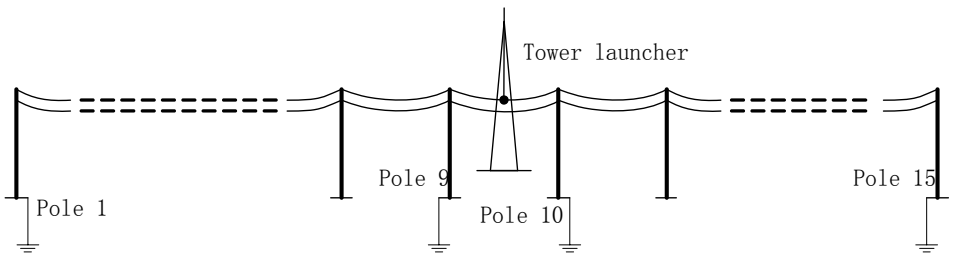

Fig 5.7 Overview of the facility for a triggered-lightning experiment

The interaction of lightning with the overhead line was modeled using EMTP. Two overhead line models were used in the simulation, in both models, the overhead line was divided into four sections shown in Fig 5.8.

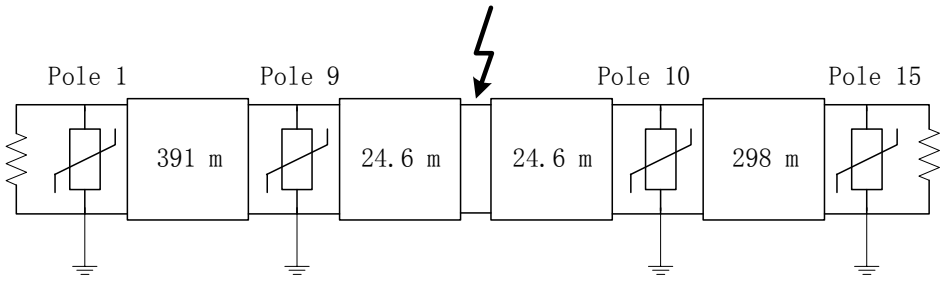

Fig 5.8 Transmission line sections used in the model

For the leads connecting the neutral to ground rods, the capacitance and inductance each per unit length of a vertical wire above ground in the absence of other conductors nearby are given by:

$$C = \frac{2\pi\varepsilon_0}{\ln\left(\frac{2h}{r}\right)} \quad \text{(F/m)} \tag{5.16}$$

$$L = \frac{\mu_0}{2\pi}\ln\left(\frac{2h}{r}\right) \quad \text{(H/m)} \tag{5.17}$$

Where h is the height above ground and r is the conductor's radius. The ground leads are 5.5 m long, and r is approximately 4.8 mm.

In a simpler model, ground rods are modeled as resistors, in the more complex model they are modeled as distributed R-L-C circuits, as shown in Fig 5.9.

The capacitance and inductance of the ground rod are given by:

$$C = \frac{\varepsilon_r l}{18 \ln\left(\frac{4l}{d}\right)} \times 10^{-9} \tag{5.18}$$

$$L = 2l \ln\left(\frac{4l}{d}\right) \times 10^{-7} \tag{5.19}$$

Where ε_r is the relative permittivity of the soil (ε_r = 10 was used)

l is the length (approximately 24 m), and

d is the diameter of the ground rod (approximately 16 mm).

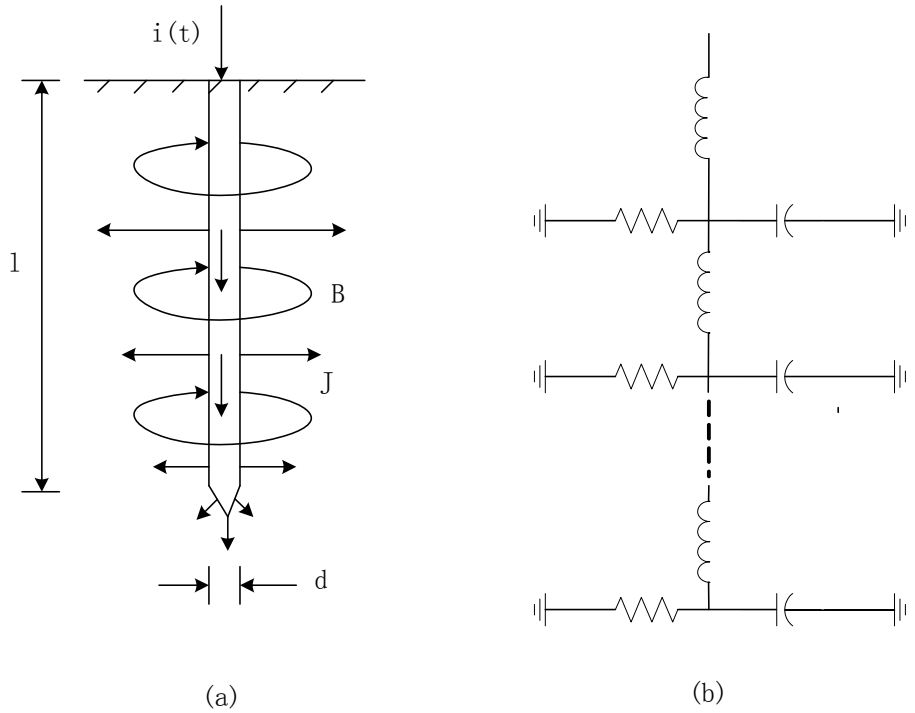

Fig 5.9 Distributed-circuit model of ground rods: (a) Schematic representation of current flow and magnetic field lines; (b) equivalent circuit of the ground rod shown in (a).

The nonlinear resistance of the ground rod is usually expressed as a function of current through the rod:

$$R_t(t) = \frac{R_0}{\sqrt{\frac{1+i(t)}{I_g}}} \tag{5.20}$$

Where R_0 is the measured low-frequency, low-current grounding resistance

i(t) is the current through the rod, and

I_g is given by:

$$I_g = \frac{E_0 \rho}{2\pi R_0^{\,2}} \tag{5.21}$$

E_0 is the critical electric field intensity (approximately 300 KV/m), and

ρ is the soil risistivity.

Using measured values of R_0 = 26 to 56 Ω, ρ = 4000 Ωm, we found that I_g is greater than 60kA. Equations (5.20) and (5.21) imply that in this system the relatively high value of ρ, relatively low values of R_0, and relatively low values of currents through the rods make the ionization of soil in the vicinity of rods unlikely.

A recorded ±13kA range of the total triggered-lightning current is employed in this simulation. Comparing the results of the measured and calculated current, the measured and calculated current to ground at pole 1, and pole 9, are in good agreement, the difference between the measured peak current at pole 1 (-2.4kA) and pole 9(-6kA) is 2.5 times, the system allows more current to be drained to ground at pole1 and 9 than at pole 10 and 15, the distribution of current to ground is mainly determined by the grounding impedance.

The measured voltage waveform at pole 1 shows initial negative spike of about 36 kV, as well as at pole 15, a plateau at 25 to 19 kV lasting for approximately 65 μs, and an

opposite polarity overshoot. The measured voltage waveform at pole 9 shows an initial negative spike clamped at 95 kV, followed by damped oscillations superimposed on a plateau that decays slowly from 30 kV to 17kV for about 29 μs. Overall, the calculated voltages with magnetic coupling modeled show better agreement with measurements than voltages computed for the other cases.

Simulations of lightning interaction with a power distribution system have been performed for different levels of complexity in the representation of the system. The impedance of the failed arrester at pole 10 appears to control the rate of flow of charge from the phase conductor to the neutral conductor and to determine mainly the duration of operation of the three operating arresters. This impedance apparently has little effect on the distribution of surges flowing to ground via the four ground rods. The initial spikes in measured voltage across the arresters have been reproduced by considering magnetic coupling to the measuring circuit. The use of the complex model is recommended if more accurate and detailed waveforms are desired; otherwise the simple model is preferred. The measured distribution of current to ground can be better reproduced by adjusting the values of grounding resistances within 50% of their measured values.

5.2.3 The Effect of Ground Conductivity on the Propagation of Lightning-Induced Voltages on Overhead Lines

Induced overvoltages are caused by the return stroke phase of a cloud to ground flash, striking in the vicinity of the overhead line. We can use a reliable coupling model to simulate the interaction of electromagnetic fields with power lines and consider the effect of propagation on the transients as they propagate along the power line.

Several coupling models have described the interaction of electromagnetic waves with overhead power lines. To derive the distribution line equations over finitely conducting ground, Vernon Cooray and Viktor Scuka [48] used an approach similar to that of Agrawal et al. [54] but modified to take into account the finite conductivity of the ground.

The relevant geometry considering a single conductor line over finitely conducting ground is shown in Fig 5.10, and the equation is obtained by

$$\begin{aligned}&\int_{-d}^{h}\left(E_z(x+\Delta x,z,\omega)-E_z(x,z,\omega)\right)dz\\&-\int_{x}^{x+\Delta x}E_x(x,h,\omega)dx+\int_{x}^{x+\Delta x}E_x(x,-d,\omega)dx\\&=j\omega\int_{x}^{x+\Delta x}\int_{-d}^{h}B_y(x,z,\omega)dxdz\end{aligned}\qquad(5.22)$$

Where d is a depth in the ground at which the amplitude of the electric and magnetic fields can be assumed to be zero.

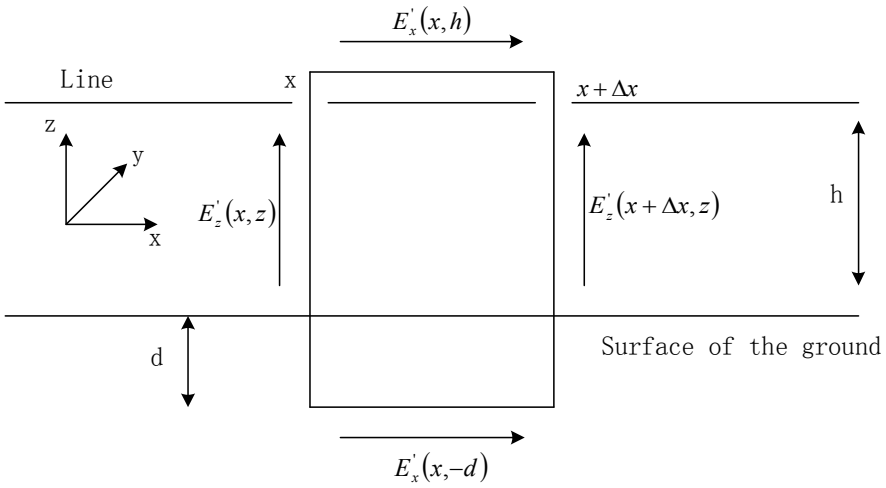

Fig 5.10 Geometry relevant to the interaction of electromagnetic fields with power lines

It is reasonable to neglect the vertical electric field in the ground, dividing each term in (5.22) by Δ x and taking the limit as Δ x $\rightarrow$ 0, it can be shown:

$$\frac{\partial}{\partial x}\int_{0}^{h}E_z(x,z,\omega)dz-E_x(x,h,\omega)=j\omega\int_{-d}^{h}B_y(x,z,\omega)dz\qquad(5.23)$$

Furthermore they deduced the transmission line equations:

$$\frac{\partial V^s(x,\omega)}{\partial x} + [R + j\omega L']I(x,\omega) = E_x^i(x,h,\omega) \tag{5.24}$$

$$\frac{\partial I(x,\omega)}{\partial x} + j\omega C V^s(x,\omega) = 0 \tag{5.25}$$

The total voltage on the line is the sum of the voltage due to the incident and scattered waves, that is shown by:

$$V^t(x,\omega) = V^s(x,\omega) - \int_0^h E_z^i(x,z,\omega)dz \tag{5.26}$$

Farhad Rachidi, Carlo Alberto and Carlo Mazzetti [47] extended the formulation proposed by Agrawal et al to the case of a wire above an imperfectly conducting ground. The coupling equations in the frequency domain can be written as:

$$\frac{dV^s(x)}{dx} + Z' I(x) = E_x^e(x,h). \tag{5.27}$$

$$\frac{dI(x)}{dx} + Y' V^s(x) = 0 \tag{5.28}$$

Where I (x) and $V^s(x)$ are the induced line current and the scattered voltage, respectively, $E_x^e(x,h)$ is the horizontal component along the wire of the exciting electric field, and Z' and Y' are the longitudinal and transverse per-unit-length impedance and admittance respectively. The transmission line (5.27) and (5.28) predict that the incident lightning electromagnetic fields excite freely propagation waves at each conductor segment.

The total induced voltage is obtained from the following equation

$$Z' = j\omega L' + Z'_{\omega} + Z'_g \tag{5.29}$$

Where $Z_{\omega}^{'}$ and $Z_{g}^{'}$ are the wire and the ground impedances, respectively. For typical overhead power and telecommunication lines and within the frequency range of interest, the wire impedance can be neglected as regard to the ground impedance. L' is the external per-unit-length inductance calculated for a lossless wire above a perfectly conducting ground

$$L^{'} = \frac{\mu_0}{2\pi}\cosh^{-1}\left(\frac{h}{a}\right) \cong \frac{\mu_0}{2\pi}\ln\frac{2h}{a} \qquad \text{for } h \gg a \tag{5.30}$$

Where h and a are the wire's height and radius, respectively.

The transverse per-unit-length admittance Y' is given by

$$Y' = \frac{(G' + j\omega C')Y_g^{'}}{G' + j\omega C' + Y_g^{'}} \tag{5.31}$$

Where C' is the per-unit-length transverse capacitance calculated for a lossless wire above a perfectly conducting ground, is given by

$$C' = \frac{2\pi\varepsilon_0}{\cosh^{-1}(h/a)} \cong \frac{2\pi\varepsilon_0}{\ln\left(\frac{2h}{a}\right)} \qquad \text{for } h \gg a \tag{5.32}$$

G' is the per-unit-length transverse conductance, given by

$$G' = \frac{\sigma_{air}}{\varepsilon_0} C' \tag{5.33}$$

And $Y_g^{'}$ is the so-called ground admittance, given by

$$Y_g^{'} \cong \frac{\gamma_g^2}{Z_g^{'}} \tag{5.34}$$

Where γ_g is the propagation constant in the ground defined as

$$\gamma_g = \sqrt{j\omega\mu_0\left(\sigma_g + j\omega\varepsilon_0\varepsilon_{rg}\right)} \tag{5.35}$$

The presence of an imperfectly conducting ground is included in the coupling equations by means of two additional terms: the longitudinal ground impedance and the transverse ground admittance, which are both frequency-dependent. The latter can generally be neglected for typical overhead lines, due to its small contribution to the overall transverse admittance of the line. Several authors have dealt with ground impedance $Z_g^{'}$ as shown below:

In 1926, Carson [24] dealt with the problem of propagation along a transmission line composed of a wire above an imperfectly conducting ground. The ground impedance can be viewed as a correction factor to the line longitudinal impedance when the ground in not a perfect conductor and it can be defined as

$$Z_g^{'} = \frac{j\omega\int_{-\infty}^{h} B_y^s(x,z)dx}{I} - j\omega L^{'} \tag{5.36}$$

Where $L^{'}$ is defined by (5.30)

$B_y^s(x,z)$ is the y-component of the scattered magnetic induction.

Sunde, neglecting the vertical component of the scattered field inside the ground, derived the following expression for the ground impedance [55].

$$Z_g^{'} = \frac{j\omega\mu_0}{\pi}\int_0^{\infty}\frac{e^{-2hx}}{\sqrt{x^2+\gamma_g^2}+x} \tag{5.37}$$

Where γ_g is defined by (5.35)

It is worth noting that a similar expression for the ground impedance had been derived earlier by Carson [24] but assuming a low frequency approximation ($\sigma_g \gg \omega\varepsilon_0\varepsilon_{rg}$)

In 1949, Sunde [55] proposed an approximation for the ground impedance given by:

$$Z_g^{'} = \frac{j\omega\mu_0}{2\pi}\ln\left(\frac{1+\gamma_g h}{\gamma_g h}\right) \tag{5.38}$$

Gary [56] presented a method that the ground was replaced with a perfectly conducting ground plane located at a complex depth d below the actual ground surface, the expression for the ground impedance was given by:

$$Z_g^{'} = \frac{j\omega\mu_0}{2\pi}\ln\left(1+\frac{1}{\sqrt{j\omega\mu_0\sigma_g h}}\right) \tag{5.39}$$

Considering the ground as a lossy cylindrical conductor surrounding a wire, Vance [57] presented a formula for the ground impedance as below:

$$Z_g^{'} = -\frac{j\gamma_g}{2\pi h\sigma_g}\frac{H_0^{(1)}\left(j\gamma_g h\right)}{H_1^{(1)}\left(j\gamma_g h\right)} \tag{5.40}$$

In which $H_0^{(1)}$ and $H_1^{(1)}$ are Hankel functions.

Chen and Damrau [58] compared the Sunde (5.38) and Vance (5.40) approximations to the general solution and concluded that both these approximations yielded accurate results.

We have presented a comparison between several approximations of the ground impedance and shown that: If the appropriate form of ground impedance expression is not used, we recommend the use of Sunde or Vance, in agreement with conclusions reported by Chen and Damrau. The Complex Plane approximation could be used in lightning-induced voltage calculations for ground conductivities not lower than about 0.001 S/m. This approximation fails for lower ground conductivities, or for faster transient source.

The field-to-transmission line coupling equations presented in the frequency-domain in (5.27) (5.28) can be converted into a time-domain. The coupling equations according to Agrawal et al. formulation in time-domain are shown below:

$$\frac{\partial v^s(x,t)}{\partial x} + L^{'}\frac{\partial i(x,t)}{\partial t} + \int_0^t \xi^{'}(t-\tau)\cdot\frac{\partial i(x,\tau)}{\partial \tau}d\tau = E_x^e(x,h,t) \tag{5.41}$$

$$\frac{\partial i(x,t)}{\partial x} + G^{'}v^s(x,t) + C^{'}\frac{\partial v^s(x,t)}{\partial t} = 0 \tag{5.42}$$

In which $\xi'(t)$ is the inverse Fourier transform.

Timotin derived the inverse Fourier transform $\xi'(t)$, the so-called ground transient resistance is given by

$$\begin{aligned}\xi'(t) &= F^{-1}\left\{\frac{Z_g'}{j\omega}\right\} \\ &= \frac{\mu_0}{\pi\tau_g}\left[\frac{1}{2\sqrt{\pi}}\sqrt{\frac{\tau_g}{t}} + \frac{1}{4}\exp(\tau_g / t)\,erfc\left(\sqrt{\frac{\tau_g}{t}}\right) - \frac{1}{4}\right]\end{aligned} \tag{5.43}$$

In which $\tau_g = h^2\mu_0\sigma_g$ and erfc is the complementary error function defined as

$$erfc(x) = \frac{2}{\sqrt{\pi}}\int_x^\infty e^{-t^2}\,dx \tag{5.44}$$

Considering a 5 km long line the calculation of lightning-induced voltages was performed for three cases shown in Fig 5.11 [47]. It can be seen that, the surge attenuation along the line can not be negligible and the induced voltages are appreciably affected by the ground conductivity through both radiated field and surge propagation along the line.

Lightning-induced voltages on power distribution or telecommunication lines have been an important factor for their insulation design. Observations have shown the importance of the influence of the ground conductivity on the lightning-induced voltage waveform by comparing measured and calculated lightning-induced voltage waveforms.

The influence of the ground conductivity on the surge propagation along overhead lines depends obviously on the lines length. For lines whose length does not exceed a certain 'critical' value (typically 2 km), the surge propagation along the lines is not appreciably affected by the ground finite conductivity that, therefore, can be neglected in the computation process of lightning-induced voltages.

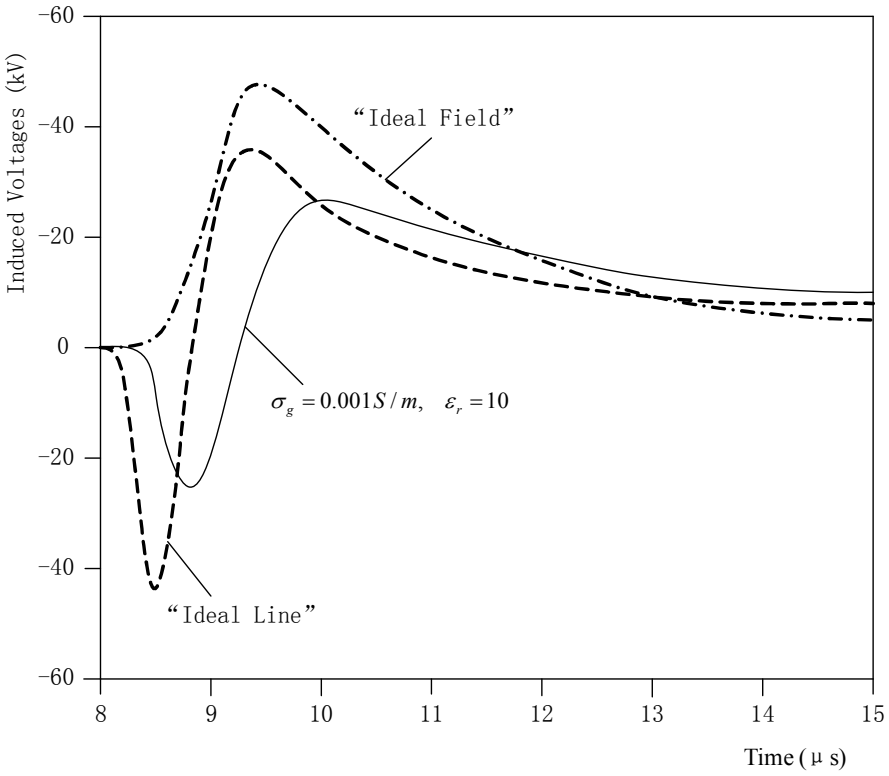

Fig 5.11 Calculated voltages on a 5-km matched overhead line induced by a typical subsequent return stroke. ($\sigma_g = 0.001 S/m, \quad \varepsilon_r = 10$).

Dashed line ("Ideal Line"): induced voltage calculated taking into account the ground finite conductivity only when calculating the exciting electric field, neglecting the ground impedance. Dotted line ("Ideal Field"): results obtained when the effect of the finite ground conductivity is taken into account only on the surge propagation along the line.

Magnitudes of lightning induced voltages for an infinitely long line increase for lower ground conductivity due to the effect of this parameter on the horizontal electric field coupling with the line. The expected number of faults due to these overvoltages increases for lines located over low conductivity grounds.

One of the notable characteristics of induced voltages influenced by the finite ground conductivity is that the voltage peak varies considerably along a wire, this characteristic

is prominent in the case that a return stroke is close to an end of a line of finite length and the polarities of the induced voltage at both ends are often opposite to each other. The crest value of the lightning-induced voltage waveform at the end of the line is greatly affected by the ground conductivity and the lightning striking points.

5.3 The Effect of SPDs on Surge Propagation

Surge protection device: A device that is intended to limit transient overvoltages and divert surge currents. It contains at least one nonlinear component [32].

5.3.1 The Characteristics of SPDs

The following characteristics are required of SPDs on LV power networks:

- Lightning strokes have large current magnitudes and hence high energy content. Therefore, SPDs which may be exposed to direct lightning strikes need high energy-handling capability.

- Strokes of both positive and negative polarity occur. Therefore, SPDs need to be able to survive and divert surges of both polarities.

- Most lightning strokes consist of more than one discharge, and hence SPDs must be able to survive multiple operations.

5.3.2 The Function of an SPD

From the Table 2.1, areas with high lightning flash density, e.g. Giant's Castle, would be expected to have more surges on the power cables than areas with low lightning flash density, e.g. Cape Town, the installation of SPDs would be affective to decrease the destruction to the power system in the high lightning flash density areas.

The purpose of installing SPDs is to provide equipotential bonding during transient conditions between live and earthy parts of an electrical system/equipment and therefore protect it from undesired transient overvoltages and to divert lightning and surge current away from it.

5.3.3 Surge Arresters

The two types of surge arresters will be considered: Gapped (Si C) and gapless (ZnO).
The voltage-current characteristic of the gapless surge arrester ZnO is reflected in a flat-topped clamping of the surge amplitudes shown in Fig 5.12. For gapped arrester the sparkgap has an inherent delay in sparkover, which gives this type of arrester an initial overshoot. Thus the gapped arrester appears to be a poor choice.

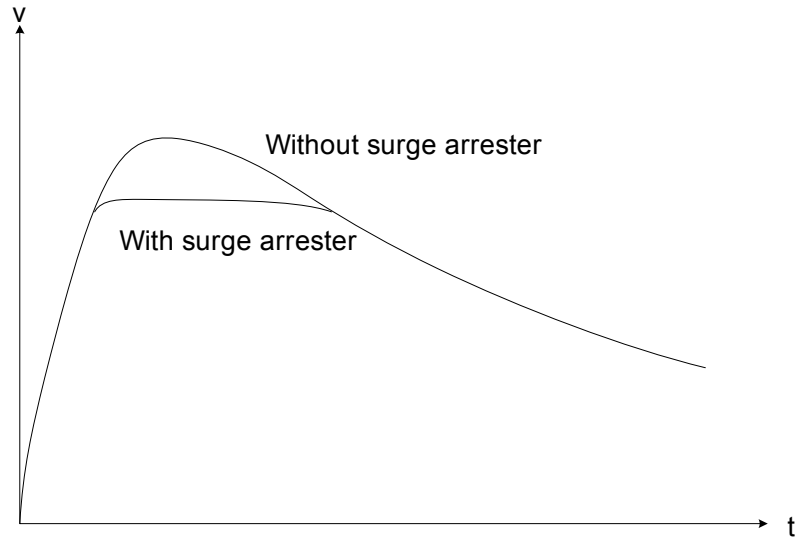

Fig 5.12 The surge characteristic of a ZnO surge arrester

5.3.4 The Selection of SPDs

If the design objective is to provide protection for a direct stroke to the building, the SPDs must be selected with sufficient current-handling capability to survive the surges resulting from the lightning surge.

The selection of the SPD depends on the expected lightning current. The selected SPDs should have a lower voltage protection level in order to provide sufficient surge overvoltage protection.

5.3.5 The Location of SPDs

The surge arrester must be mounted as close to the transformer as possible (to avoid large inductive voltages along the surge arrester leads when the surge current through the surge arrester increases rapidly)

For a low voltage distribution system, when lightning strikes the external LPS of a building, there is a high potential difference between the phase and neutral conductors. By providing equipotential bonding between earthed and live conductors through SPDs this high potential difference can be reduced. But due to the conduction of the SPDs, partial lightning current flows through them towards the transformer site via the phase and neutral conductors [11].

A direct lightning strike to a building can produce high stresses on the service entrance SPDs, SPDs in that building will be strongly affected, while nearby buildings will be impacted by much lower surge currents.

In a TN system where the neutral is bonded to earth at the service entrance, there is no SPD in that path, and thus no concern about neutral SPD integrity. In typical residential single-phase U.S. systems, the line SPDs can carry about 25% of the strike current [37].

5.4 Summary

The process of surge propagation and the affecting factors have been introduced. The models and formulas related to surge propagation have been presented. The theory and equations on the influence of ground conductivity on lighting-induced voltages on an overhead wire have been presented both in frequency and time domains

When a lightning strikes MV distribution lines, the large surges occur and can be transferred down to LV consumers through a distribution transformer. Typically, 50% of the amplitude of a lightning surge can be transferred across a transformer [36].

The lightning transient performance of an earth electrode differs significantly from the power frequency performance. The ionization and propagation footing model provides a reasonable match to experimental studies of footing response under lightning surge conditions. It is recommended that the combined model can be used for calculating lightning outage rates. The surge impedance of the earth electrode of a transmission line depends on the geometry of the buried electrode system and the soil resistivity.

In simulation of lightning surge propagation interacting with a power distribution system, the use of a complex model is recommended if more accurate and detailed waveforms are desired, otherwise a simple model is preferred. When measuring low-frequency, low-current grounding resistances, the relatively high value of soil resistivity, low values of resistance, and relatively low values of currents make it impossible to ionize the soil in the vicinity of earth electrodes.

Lightning-induced voltages on power distribution or telecommunication lines have been an important factor for their insulation design. Observations have shown the importance of the influence of the ground conductivity on the lightning-induced voltage waveform by comparing measured and calculated lightning-induced voltage waveforms.

The influence of the ground conductivity on the surge propagation along overhead lines depends obviously on the lines length. For lines whose length does not exceed a certain ‘critical’ value (typically 2 km), the surge propagation along the lines is not appreciably affected by the ground finite conductivity which, therefore, can be neglected in the computation process of lightning-induced voltages.

Magnitudes of lightning-induced voltages for an infinitely long line increase for lower ground conductivity due to the effect of this parameter on the horizontal electric field coupling with the line. The expected number of faults due to these overvoltages increases for lines located over low conductivity grounds.

In the protection of a distribution system against lightning surge propagation, SPDs, especially gapless surge arresters play a very important role. They can balance the potential difference between the live and earthy parts of the electrical system.

Chapter 6

SURGE ATTENUATION

This chapter introduces the possible approaches for attenuating surges and the effect of soil resistivity during the process of surge attenuation. The forms of earth electrodes and related models are analyzed specifically, and the effects of soil ionization are also included. This chapter also provides the impedance formulas relative to soil resistivity for earth electrodes in both ionized and non- ionized soil.

6.1 Surge Attenuation

6.1.1 Transmission Line Footing

Lightning currents injected into ground electrodes of transmission network footing can cause non-linear ionization and attenuation of transient. Electrode shape, soil resistivity, ionization are major factors affecting the surge attenuation.

6.1.2 LPZ

In SABS IEC 1312-1 (1995) [2] Lightning protection zone (LPZ) is defined that zones where lightning electromagnetic environment is to be defined and controlled.

Zone definitions are:

- LPZ O_A: Zone where items are subject to direct lightning strokes, and therefore may have to carry up to the full lightning current. The unattenuated electromagnetic field occurs here.

- LPZ O_B: Zone where items are not subject to direct lightning strokes, but the unattenuated electromagnetic field occurs.

- LPZ 1: Zone where items are not subject to direct lightning strokes and where currents on all conductive parts within this zone are further reduced compared with zones O_B. In this zone the electromagnetic field may also be attenuated depending on the screening measures.

- Subsequent zones (LPZ 2, etc): If a further reduction of conducted currents and electromagnetic field is required, subsequent zones shall be introduced. This part should be ignored due to the scope of this research report based on the domestic application.

At the boundary of the individual zones, bonding of all metal penetrations is provided and screening measures can be installed. Fig 6.1 shows an example for dividing a house (building) into several zones.

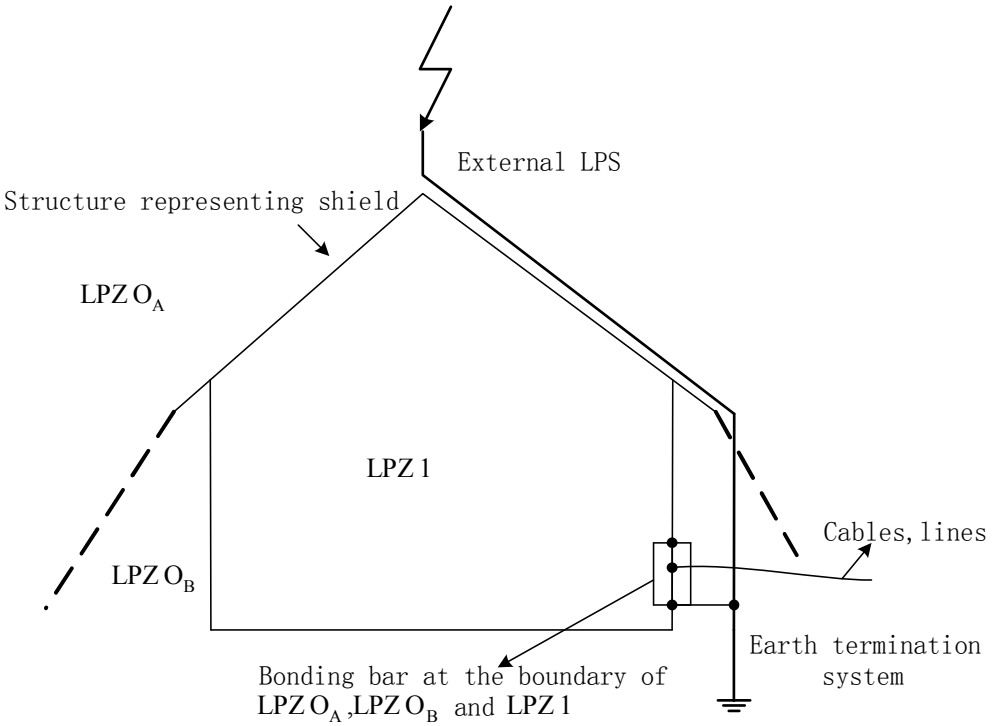

Fig 6.1 An example for diving a house into several LPZs

The maximum surge voltages at the boundary of the LPZ should be coordinated with the withstand capability of the systems involved. An unavoidable consequence of bonding and equipotentiality is the flow of partial lightning currents throughout the common earthing system which can couple with nearby signal and power cables if adequate shielding is not provided, resulting in potentially damaging overvoltages [31].

In the bonding elements, only a minor proportion of the lightning current is expected to flow. Between the different zones of LPZ, the surge is expected to be attenuated from the LPZ O_A to subsequent zone.

6.1.3 Earthing

An earth electrode consists of one or more conductors buried in the earth that provide a mechanism for the dispersal of either fault or lightning current into the earth. Earthing plays the significant role in the lightning surge attenuation.

When transient currents, as in the case of lightning discharge currents, have to be dissipated, the transient impedance characteristic becomes a variable parameter depending upon the frequency content and the magnitude of the current.

6.2 The Effect of Soil Resistivity

6.2.1 Footing Resistance

Lightning surge attenuation on overhead transmission line is strongly affected by the footing resistance, a typical transmission line fault caused by lightning is shown in Fig 6.2.

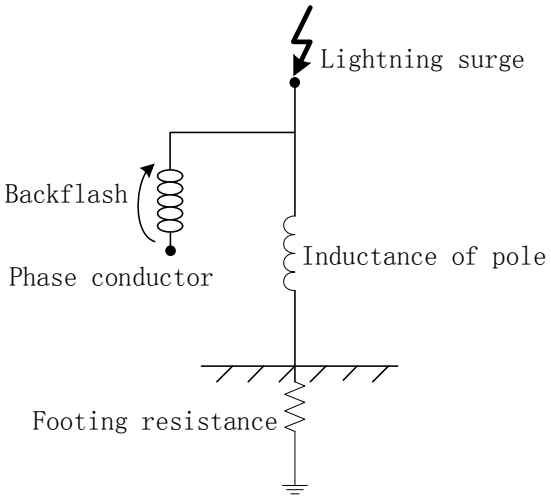

Fig 6.2 A typical transmission line fault caused by lightning

In a transient the voltage drops and the resultant voltages will be determined by the impedance of the line and will thus be primarily affected by its reactance. The resistance will affect the losses only and thereby the attenuation of the natural component of the transient, this attenuation is very small.

In an attempt to examine the effect of the generally poorly known ground resistivity on transmission line transients, Adam Semlyen [16] found that a 1% variation in soil resistivity may result in a nearly 0.5% change in some features of a transient, such as surge attenuation.

6.2.2 Earthing Electrodes

The first researchers who attempted to model the dynamic impedance of an electrode were Bellaschi, Armington and Snowden in 1942. They described the impedance of an electrode in terms of a uniform ionization zone which was said to surround the electrode whenever the critical breakdown strength, E_0, of the soil was exceeded. This principle has since then formed the basis of almost all the subsequent models which attempt to

predict the impedances of electrodes in soil when ionization and discharge processes are involved [30].

6.2.2.1 The Forms of Earth Electrodes

In designing an earthing system, the following types of earth electrodes shall be considered: one or more ring (or trench) electrodes, vertical (or concentrated) electrodes, grid electrodes, or a foundation earth electrode, and site-wide earth electrodes.

A concentrated earth electrode is distinguished from a distributed electrode by the physical dimension of the electrode being small in comparison with the wavelength of the highest frequency components of lightning current. A grid electrode consists of a significant array of conductors buried below ground level whose primary purpose is that of safety-limiting touch-and step-potentials and dispersing power frequency fault currents to earth. A site-wide earth electrode system is composed of one or more of the other types of earth electrode that are interconnected and form part of the equipotentiality and bonding network.

6.2.2.2 The Impedance Characteristics of Earth Electrodes

In the case of a design that has to take transient discharges into account, the following objectives must be satisfied:

- A low surge impedance, which is the initial earth impedance of the electrode under transient condition.

- A low leakage resistance, which is the low-frequency earth resistance of the electrode after the transient discharge has been dissipated and which refers to a steady-state condition of low current.

The actual impedance characteristics during the change from surge impedance to leakage resistance are complex and are further complicated by ionization effects in the soil

Earth electrodes exhibit different impedance characteristics for current of different magnitudes and frequencies. Trench electrodes are known to offer lower impedance at power frequency than do equivalent vertical conductors. Vertical rods offer superior performance under surge conditions.

Factors influencing the dynamic impedance of earth electrodes are:

- The impedance of the electrode itself, a concentrated earthing system is one in which the impedance of the electrode itself is negligible.

- The frequency-dependent electrical properties, ε, and ρ, of the soil.

- The ionization and discharge processes in soil.

6.2.2.3 Basic Formulas

When a lightning current is discharged into a buried conductor, the electric field in the soil surrounding the conductor can be found by

$$E = J.\rho_{soil} \text{ (V/m)} \qquad (6.1)$$

Where

E = electric field (V/m)

J = current density (A/m^2)

ρ_{soil} = soil resistivity (Ω m)

From the electric field in the soil we can derive the voltage of the earth electrode, V, by integrating over distance from the earth electrode

$$V = \int E dx = \int J \cdot \rho_{soil} dx \tag{6.2}$$

Finally dividing this voltage by the total lightning current we get the earth resistance, R_g, where

$$R_g = \frac{V}{I} = \frac{1}{I} \int J \cdot \rho_{soil} dx \tag{6.3}$$

The value of R_g is a strong function of the geometry of the buried earth electrode.

6.2.2.4 Soil Ionization

Ionization is said to occur in soil where E exceeds a critical value, E_0, resulting in an increase in effective conductor dimensions and therefore a lowering of apparent resistance to earth seen by the current source.

The soil breakdown mechanism described above implies that quantity E_0 should exhibit the following characteristics:

- E_0 for any soil will always be less than of the air.
- E_0 should drop with increase in water content because of the resulting increase in the dielectric constant of the soil.
- For the same water content, soils having very fine grains should have somewhat higher values of E_0 compared to soils having medium or coarse grains.

- That soil resistivity is high then E_0 would also be high is not valid, because E_0 is governed by ionization of the air in the voids while soil resistivity is governed by flow of current in the water which coats the soil particles.

6.2.3 Concentrated Earth Electrode

6.2.3.1 The Process of Ionization

A dynamic model proposed by Liew& Darveniza (1974) [43] was chosen to represent the impulse behaviour of a concentrated earth electrode. In this model, the full non-linear effects of ionization in the surrounding soil are accounted for by introducing two time constants, to describe the changing resistivity in the surrounding soil under impulse conditions.

A typical profile of the dynamically changing resistivity proposed by Liew& Darveniza (1974) can be seen in Fig 6.3. From this Fig, there is no ionization and the resistivity remains constant at first. Once the critical current density has been exceeded, the resistivity then decreases to a minimum value with increasing current density, after which it recovers as the soil deionization. The non-linear behaviour and hysteresis is distinct.

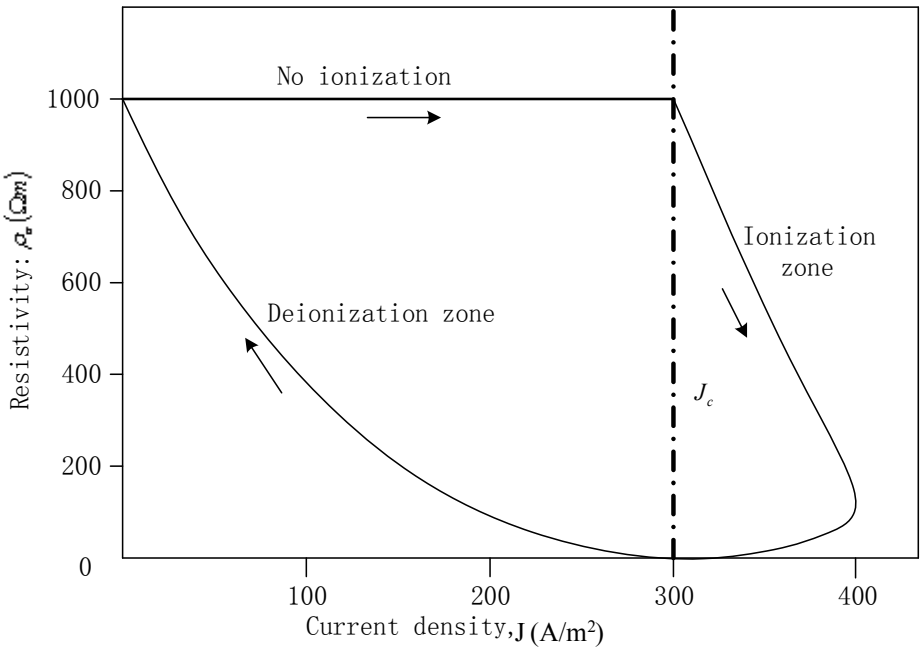

Fig 6.3 Resistivity profile proposed by Liew and Darveniza

6.2.3.2 The Model of Ionization

In the case of a hemispherical electrode, the ionized zone would be a hemisphere as shown in Fig 6.4 [15].

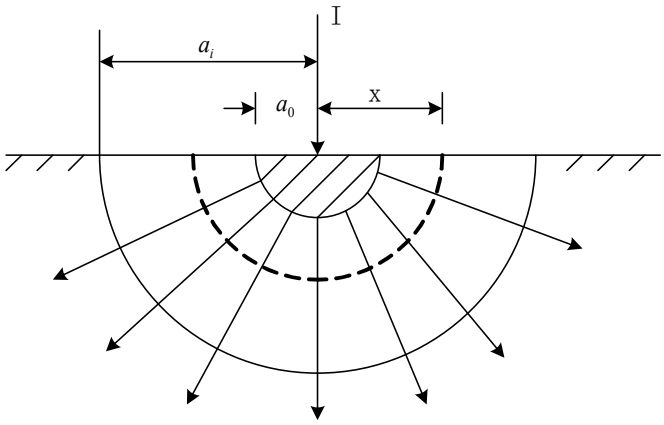

Fig 6.4 The model of hemispherical electrode ionized

For a single driven rod of length l_0 and radius r_0, Nixon [31] adopted the Liew's vision that took the ionized zone to be of the form shown in Fig 6.5, the following assumptions are made:

- The soil surrounding the driven rod is homogeneous and isotropic with resistivity ρ_{soil}

- An injected impulse current I results in equipotential surfaces that can be approximated by a cylindrical and hemispherical portion, as shown in Fig 6.5.

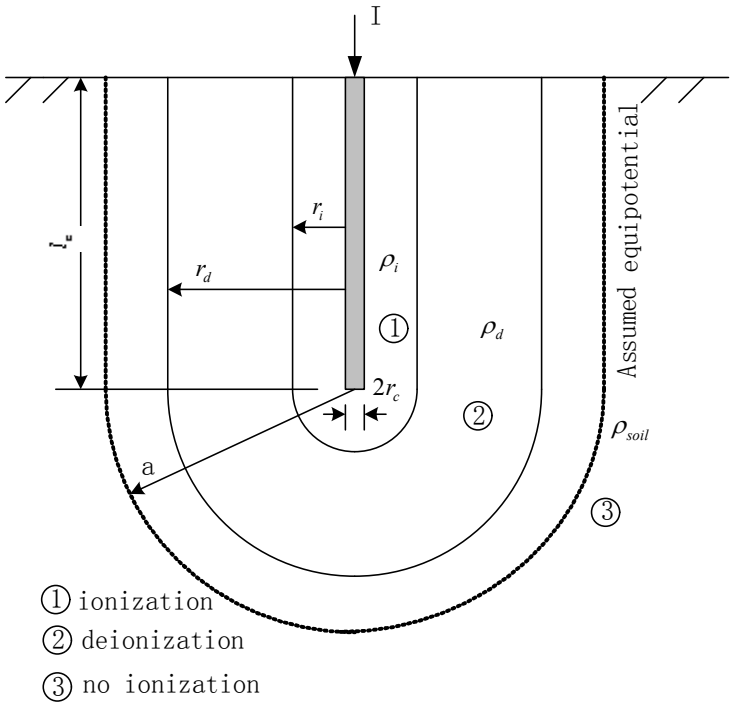

Fig 6.5 Simplified model of a single driven rod showing the ionization and deionization zones

- The current density, J , in the soil at a radial distance, a ,from the centre of the driven rod can be approximated by:

$$J = \frac{I}{2\pi a\left(a + l_0\right)^2} \qquad \left(A/m^2\right) \tag{6.4}$$

- Breakdown by ionization occurs in the soil where the current density exceeds a critical value of current density, J_c, given by:

$$J_c = \frac{E_0}{\rho_{soil}} \qquad \left(A/m^2\right) \tag{6.5}$$

- The regions of ionization and deionization are assumed to be uniform as shown in Fig 6.5 and the resistivity in these regions is time varying.

6.2.3.3 The Effective Resistance of a Driven Rod

Using the assumptions listed in the previous section, Liew & Darveniza (1974) [43] determined the effective resistance of a single driven rod R_{rod}, by summing elemental shells of resistance, dR, given by:

$$dR = \frac{\rho_a}{2\pi l_0}\left(\frac{1}{r} - \frac{1}{a + l_0}\right)da \qquad (\Omega) \tag{6.6}$$

Where

t_i = time since the onset of ionization [s]

τ_i = ionization time constant [s]

These elemental shells fall into three distinct regions as shown in Fig 6.5:

Region 1. Where ionization is occurring, $J \geqq J_c$ and $r_o < a \leqq r_i$.

The resistivity of the soil in this region ρ_i is given by:

$$\rho_i = \rho_{soil} \exp\frac{-t_i}{\tau_i} \qquad (\Omega m) \tag{6.7}$$

Where

t_i = time since the onset of ionization (s)

τ_i = ionization time constant (s)

Region 2. Where residual activity exists (deionization), $J < J_c$ and $r_i < a < r_d$.

The resistivity of the soil in this region ρ_d is given by:

$$\rho_d = \rho_m + (\rho_{soil} - \rho_m)\left(1 - \exp\frac{-t_d}{\tau_d}\right)\left(1 - \frac{J}{J_c}\right) \quad (\Omega m) \tag{6.8}$$

Where

ρ_m = value of resistivity at onset of deionization given by Equation 6.7 (Ωm)

t_d = time measured from the onset of deionization [s]

Region 3. Where the resistivity is constant, $J < J_c$ and $a > r_d$.

In this region resistivity is that of the surrounding soil ρ_{soil}.

The effective resistance, R_{rod}, can be calculated by summing the resistances of the three regions as below:

$$R_{rod} = \frac{\rho_i}{2\pi l_0}\ln\frac{r_i(r_0 + l_0)}{r_0(r_i + l_0)} + \frac{\rho d}{2\pi l_0}\ln\frac{r_d(r_i + l_0)}{r_i(r_d + l_0)} + \frac{\rho_{soil}}{2\pi l_0}\ln\frac{r_d + l_0}{r_d} \qquad (\Omega) \tag{6.9}$$

When no ionization exists, the low current, or leakage resistance is given by:

$$R_{rod0} = \frac{\rho_{soil}}{2\pi l_0}\ln\frac{r_0 + l_0}{r_0} \qquad (\Omega) \tag{6.10}$$

The portion of the soil in the immediate vicinity of the electrode generates a large portion of the total resistance because the cross section of flow of current in that zone is small. This is shown in Table 6.1 and Table 6.2 [15] for the cases of a hemispherical electrode (Fig 6.4) and a driven rod (Fig 6.5), respectively. It follows that shorting out a part of the soil in that zone would significantly reduce the grounding resistance.

Table 6.1 Contribution of the soil in the immediate vicinity of a hemispherical electrode to its total resistance

x/a_0	2	3	4	5	10	50	∞
% Resistance	50	66.7	75	80	90	98	100

Table 6.2 Contribution of the soil in the immediate vicinity of a ground rod to its total resistance

r_i/L_c	0.1	0.25	0.5	1.0	2.0	5.0	∞
% Resistance	58.3	72.0	80.9	87.9	92.9	96.8	100

The dynamic model (Fig 6.5) implemented shows satisfactory agreement with experimental result. Using the model can quantify the effect of soil ionization and impulse current magnitude on the minimum dynamic resistance of a driven rod for different impulse current magnitudes.

6.2.3.4 Selection of Model Parameters

Because of the lack of sufficient information, the values for the ionization time constants, τ_i and τ_d, have been taken to be 2 μs and 4.5 μs respectively.

Usually, the value of E_0 was chosen to fit theoretically predicted results to experimental results. Mousa claimed that E_0 be taken equal to 300 KV/m for typical soils [15]. Oettle

[30] recommended approximating E_0 as 10 kV/cm due to the inherent complexity of the discharge processes in the soil and suggested that experimental breakdown test results not be used, even if available.

Higher values of E_0 cause the effects of soil ionization to be slightly less marked since the ionization zone does not extend as far from the driven rod as for lower values. Therefore, the higher value of 10 KV/cm recommended by Oettle would result in slightly conservative predictions made by the model.

Another parameter that can vary quite considerable is the prevailing soil resistivity ρ_{soil}. In most cases, a standard Wenner method [4] can be used to obtain a depth profile of the soil resistivity on-site. If layers of different soil resistivity exist, which is quite common in South Africa, the soil resistivity can be obtained by Blattner methods [17]

6.2.3.5 Limitations and Premises in the Model

The important limitations and the premises of the modeling that exist are discussed below.

- The model described and implemented is applicable only for a single driven rod. The model can be extended to multiple driven rods if necessary.

- The surrounding soil is assumed to be homogeneous in order to use single defined values for E_0 and ρ_{soil} in the model. As a result, multiple layers of resistivity in the soil can only be considered by approximating the layers as one layer.

- The breakdown process is assumed to result in a uniform zone of ionization that extends a certain radius from the surface of the driven rod as opposed to the non-uniform breakdown paths.

- The model is only valid for the electrode performance at typical lightning impulse current frequencies and will lose accuracy at frequencies above 1 MHz since the frequency-dependent electrical properties of soil ignored in the model.

- In most cases, the self-inductance of the driven rod can be ignored, but in some installations deep-driven rods are used and in this case it is important to include the self-inductance of the rod.

6.2.3.6 Conclusion

The model of a driven rod accounts for the non-linear effect of soil ionization and can predict the dynamic resistance of a driven rod based on the current injected through the rod. The model was used to produce a theoretical prediction of the impulse response of a driven rod and showed good agreement with results obtained experimentally.

Using the model, the effect of soil ionization shows a significant decrease in the effective resistance of a driven rod under impulse conditions. This decrease is typically in the range of 20% to 80% of the low current resistance value. For increasing current magnitudes, the decrease in effective electrode resistance tends towards a limiting value. It was concluded that the effects of soil ionization are significant and must be included when modeling concentrated earth electrode.

If the effect of soil ionization is ignored, the driven rod performs exactly the same under transient conditions as under DC conditions. However, if soil ionization is included the driven rod performs significantly better for all soil conditions under transient conditions; Soil ionization does not affect the performance of the long trench, even if the trench is in high resistivity soil. This is due to the typically large initial surge impedance of a distributed earth electrode and the soil ionization time-constant of approximately 2 μs.

6.2.4 Multiple Driven Rods

6.2.4.1 Three Point Star Structure

Electrodes constructed from a combination of driven rods and radial arrays of buried conductors are installed in order to ensure a stable resistance value and to minimize the hazard of high surface potentials during times of current discharge. Combined electrodes also satisfy the objective of having both surge impedances and 50 Hz impedances as low as possible. Combination also facilitates current division as well as offering multiple independent paths to reduce the effect of a possible earthing conductor failure.

Based on the scope of the research, in the case of distribution transformer, a three point star electrode configuration is preferred by ESKOM [8]. When a number of vertical rods buried in a straight line or star are connected in parallel by means of a buried bare conductor, the combined earth resistance is given by the Sunde equation

$$R = \frac{R_h R_d - R_m{}^2}{R_h + R_d - 2R_m} \tag{6.11}$$

Where R_h = earth resistance of total length of buried horizontal conductor alone, Ω

R_d = combined earth resistance of array of buried vertical rods alone, Ω

R_m = mutual resistance of horizontal and vertical earthing systems, Ω,

Given by

$$R_m = \frac{\rho}{\pi \cdot Lh} \cdot \ln \frac{2Lh}{L_0} \tag{6.12}$$

L_h = total buried length of the horizontal conductor, m

L_0 = buried length of each rod, m

Oettle [30] illustrated this idea of a uniform ionized zone of three point star electrodes in Fig 6.6.

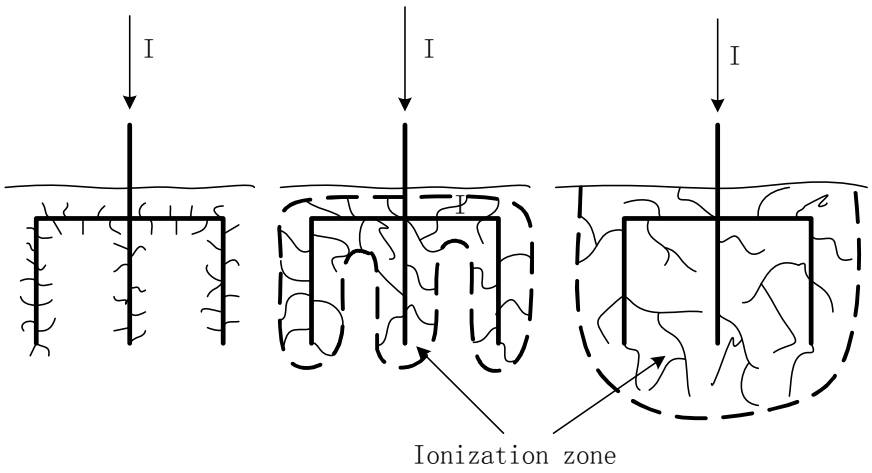

Fig 6.6 The development of a uniform ionization zone

Korsuntsev [44] based his physical model on the concept of a uniform spark zone, the boundaries of which were determined by the critical breakdown strength E_0, of the soil. Within this zone, the resistance was assumed to the zero. Thus at the ionization zone boundaries:

$$E = E_0 = \rho j \tag{6.13}$$

Where E = electrical field strength in the soil

ρ = soil resistivity

j = current density

Fig 6.6 shows that, as the current increases, the exact electrode configuration becomes less important and only the overall dimensions of the ionization zone are of major significance. Korsuntcev thus introduced the idea of a characteristic dimension, s, which is an indication of the overall dimension of an electrode. The current density around the

electrode would then be proportional to I/s^2, while the electrical field adjacent to the electrode could be represented by $\rho\ I/s^2$.

Dan Mordechai [41] tested the impulse current distribution of the star point of the electrodes which shown in Fig 6.7.

From the measurement, if the current in coil #3 was chosen as reference (100%), the impulse current in the coil #4 was about 75-90%, and the impulse current in the coil #2 was about 95-130% relative to coil #3. Under impulse conditions most of the current (75-90%) is being dissipated from the rods. Furthermore, rod # 2 is dissipating more current than rod #4.this could be attributed to the fact that rod #2 is closer to the point of current injection.

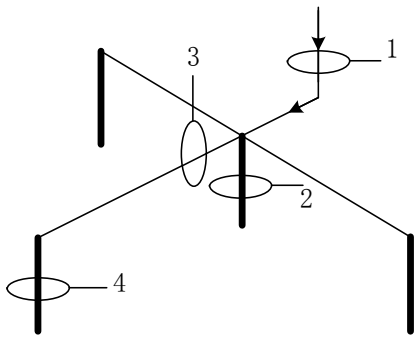

Fig 6.7 Location of coils for current distribution measurement of star point

Dan Mordechai also observed that heavy ionization was taking place around the rods rather than around the trench conductors. The soil resistivity around the rods is lower by a factor of 2 to 3 compared with around the trench conductors. Lower soil resistivity implies that for ionization to take place a higher current density is needed.

6.2.4.2 n Vertical Rods

The earth resistance of n vertical rods of equal effective length L and connected in parallel at equal spacing s in a straight line or in an open or solid square is given [4] by

$$R = R_0 \frac{1 + km}{n} = R_0 Y_n \tag{6.14}$$

Where k = the appropriate factor given

$$m = \frac{L}{\left[\ln\left(\frac{8L}{d}\right) - 1\right] s} = \frac{r_e}{s} \tag{6.15}$$

And r_e = radius of equivalent hemispherical electrode, m

Y.L.Chow [22] introduces sunken rodbed of N rods in Fig 6.8, 0 ⩽h ⩽ ι + h_b

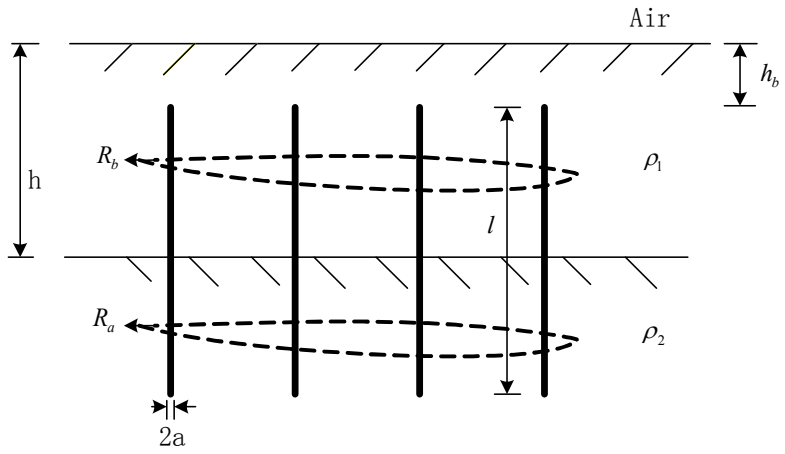

Fig 6.8 Rodbed in two-layer earth

$$R_t = \frac{1}{\frac{1}{R_a} + \frac{1}{R_b}} \tag{6.16}$$

Where R_t is the rodbed resistance,

$$R_a = \frac{\rho_2}{(l + h_b - h)} \cdot g_0 \cdot \frac{F_0}{N} \tag{6.17}$$

$$R_b = \frac{\rho_1}{(h - h_b)} g_0 \frac{F_0}{N} + \frac{\rho_1}{h} \phi_0 \tag{6.18}$$

$$g_0 = \frac{1}{2\pi} \left[\ln\left(\frac{2l}{a}\right) - 1 + \frac{\ln 2}{1 + \frac{(4 \ln 2) h_b}{l}} \right] \tag{6.19}$$

Where ι = length of driven rod and a = radius of driven rod.

The F factor of N rods in a homogeneous earth,

$$F = 1 + \left(N - \frac{1}{\sqrt{N}} \right) \frac{R_S}{RL} \tag{6.20}$$

Where R_s is the resistance of the solid sleeve with a sleeve surface area S. The multiple reflections of the two-layer earth effectively changes the rod length of each rod, then

$$F = F \Big|_{l \to \frac{l}{1-0.9K}} \tag{6.21}$$

The above arrow means the replacement of l by $l/(1-0.9K)$.

6.2.4.3 The Frequency-Dependent Properties of Soil without Ionization

Oettle [30] modeled a concentrated earthing system as shown in Fig 6.9. The resistance, R, and the capacitance, C, to ground, are determined by the frequency-dependent properties of the soil, whereas the spark gap and the variable resistance R_i, represent the reduction in the earth's impedance under high current impulse conditions when ionization and discharge processes are involved.

Under natural conditions, a wide range of soil type is encountered, with resistivities which differ greatly at different sites and with seasonal changes. Uncertainties regarding corresponding variations in the permittivity have made engineers hesitant to use these mathematical methods to assess the impulse response of electrodes. It is convenient to define a new parameter which can be called the impedancy, of the soil, such that

$$\zeta = \left(\frac{1}{\rho} + i2\pi f\varepsilon \right)^{-1} \tag{6.22}$$

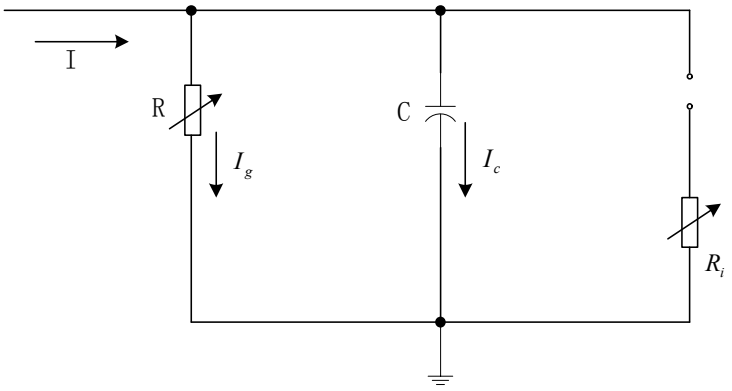

Fig 6.9 Simple lumped parameter circuit model for a concentrated earthing system

The total impedance, Z, across a soil section of length, l, and area, A, would then be given by

$$Z = \frac{l}{A} \cdot \zeta = \left(\frac{A}{\rho l} + \frac{i 2\pi f \varepsilon A}{l} \right)^{-1} \tag{6.23}$$

Which is the parallel combination of the resistance and the capacitance of the section. The impedance of an earth electrode is a function of frequency. This means that a mathematical analysis of the dynamic response of an electrode is extremely complex, calling not only for a frequency spectrum analysis of the applied impulse, but also for the frequency-dependent behavior of ρ and ε to be taken into account.

In soil, the conduction is almost entirely electrolytic, with current flow taking place through the movement of positive and negative ions dissolved in the microscopic layers of water surrounding the soil particles. This results in the most unusual frequency-dependent electrical properties of soil, as illustrated in Fig 6.10, Fig 6.10 serves to illustrate only the order or magnitude and the dispersion in the relative dielectric constant and resistivity.

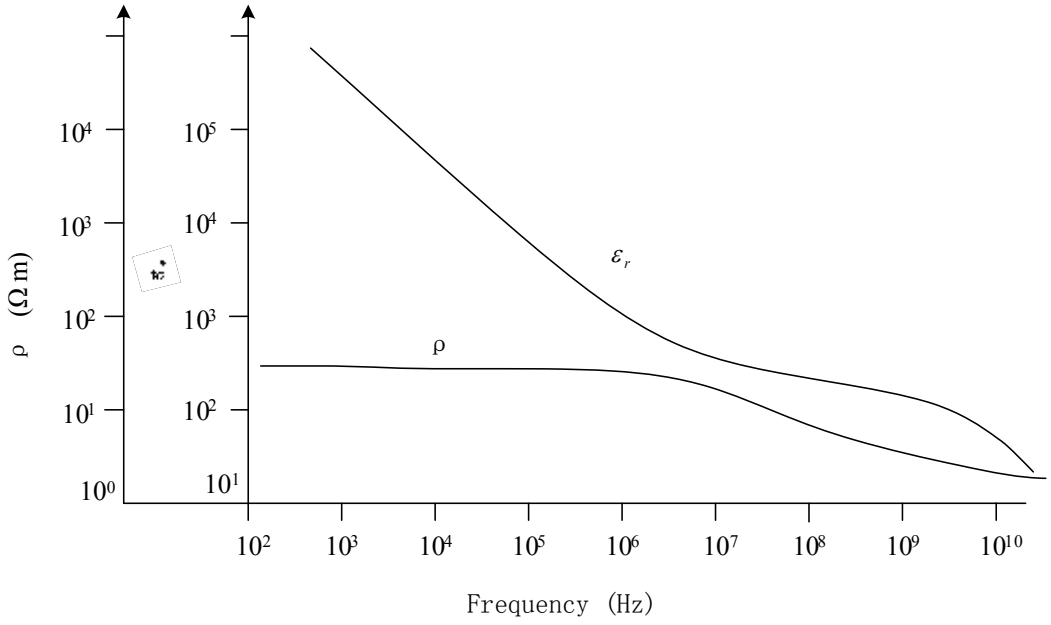

Fig 6.10 Typical values of ρ and ε_r for frequencies between 100 Hz and 10 GHz

The decrease in ρ and ζ at increasing frequencies is illustrated in Fig 6.11 for given soil sample

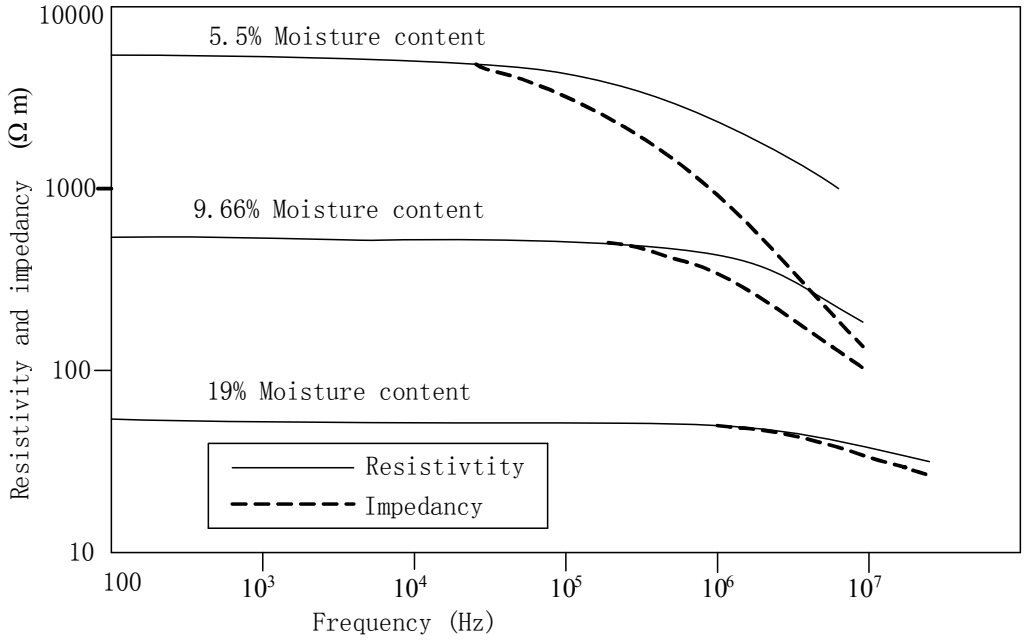

Fig 6.11 The resistivity and the impedance, plotted as a function of frequency, for given soil samples.

For very high frequencies the impedance in most soil conditions will be well attenuated. However, for lightning current waveshapes, when only frequencies of below 1 MHz are of interest, it will only be in soils with exceptionally high resistivities that the high-frequency properties can be expected to cause a notable decrease in the lightning overvoltages which develop on an electrode.

6.2.5 Concrete-Encased Earth Electrodes

6.2.5.1 Conductive Concrete Characteristics

Conductive concrete is often used in earthing application in distribution systems to decrease the resistance to true earth of transformer earthing electrode, particularly in area with high soil resistivities.

The application of conductive concrete is most effective where the resistivity of the soil, ρ_e, is greater than 100 times that of the concrete, ρ_c (i.e. $\rho_e > 100\rho_c$). Conductive concrete is less effective in more conductive soils and should not be used in cases where the soil resistivity is less than 300 Ω m [9].

Concrete below ground level is a semi-conducting medium of about 30 Ω m resistivities at 20 ºC, or somewhat lower than average earth resistivity. Consequently, in earth of average or higher resistivity, the encasement of rod or wire electrodes in concrete develops lower resistance than a similar electrode directly in earth [39].

Grid system of a building usually extends over the entire building yard and may extend some distance beyond the boundary fence. They consist of conductors buried in the ground or concrete and forming a network of squares. All the wires (reinforcing steel bars) crossings should be securely bonded and the system connected to the normal ground system as well as to all equipment and structural steel work.

6.2.5.2 The Advantage of Conductive Concrete

In a building, especially in the multilayer building, concrete is used almost universally in the footing and foundations of buildings and in the bases of structures. The concrete is inevitably in close contact with the earth over a relatively large area. Conductors, either embedded in or laid under the concrete foundations, it is possible to provide an earth electrode that has a low earth resistance, is economical to install as no trenches have to be

specially excavated, is little exposed to the drying out of soil or to seasonal variations in moisture content, is often well protected against corrosion and is inaccessible to pilfering or earth-working machinery [4].

Rebars should preferably not be used for earth fault currents but usually provide an excellent earth electrode for lightning discharge currents and have a low surge impedance as a result of the distributed capacitive effect of the foundations. Incidental contacts between rebars in splice joints from roof to foundations usually provide a low impedance path for lightning discharge currents.

It was equally important to determine the additional cost of using conductive concrete and compare that cost with an equivalent electrode using additional lengths of copper to achieve the same resistance to true earth. Conductive concrete would provide a solution to problematic areas, such as those areas in South Africa with a high soil resistivity, without increasing the cost of the electrode by more than fifty percent.

Encasing an earth electrode in conductive concrete is a costly means of reducing the electrode resistance to true earth. Encasing electrodes in concrete has the added benefit of improved resistance to theft.

6.2.5.3 The Effect of Soil Resistivity

Concrete is inherently alkaline, hygroscopic and of high density, little subject to leaching. Its resistivity depends on moisture content and may vary from 30 - 300 Ω m. Certain non-corrosive additives may further reduce the resistivity of the concrete. In moist conductive soils the ratio of the resistivities of concreter to soil tends to approach unity.

SABS 0199(1985) [4] proposed an equation for the case of an earth rod surrounding with concrete in a hole:

$$R = \frac{\rho_{concrete}}{2\pi L} \cdot \ln\left(\frac{L \cdot d_2}{H \cdot d_1}\right) + \frac{\rho_{soil}}{2\pi H} \cdot \ln\left(\frac{4H}{d_2}\right) \qquad (6.24)$$

Where

R = Resistance of concrete encased rod (Ω)

$\rho_{concrete}$ = Resistance of concrete (Ω m)

ρ_{soil} = Resistance of soil (Ω m)

L = Length of ground rod (m)

H = Depth of hole (m)

d_1 = Diameter of ground rod (m)

d_2 = Diameter of concrete filling (m)

An example was given in SABS 0199(1985) as below:

$\rho_{concrete}$ = 200 Ω m

ρ_{soil} = 1000 Ω m

L = 3 m

H ≧ 3.15 m

d_1 = 0.016 m

d_2 = 0.300 m

R was calculated to be 220 Ω, a reduction of 37%, comparing the value for which the same rod set in earth would have a calculated resistance of 350 Ω.

Darryl [42] uses the CDEGS (Current Distribution, Electromagnetic, Grounding and Soil Structure Analysis) package software to calculate resistance values on electrodes with concrete encasements of varying resistivity (both the concrete and the surrounding soil). He assumed that the diameter of the copper rod was fixed at 10 mm and had a fixed

length of 1m, the diameter of the encased rod was fixed at 150 mm and the conductive concrete was fixed at a resistivity of 1 Ω m, the results are shown in Table 6.3.

Table 6.3 Calculated resistances for varied soil resistivity

Soil resistivity (Ω m)	Without concrete (Ω)	With concrete (Ω)
1	0.93	0.93
10	9.31	5.39
100	93.05	49.42
200	186.09	98.39
300	279.14	147.37
1000	930.46	490.20

From the above results the effect of the conductive concrete increases with increasing soil resistivity up to the point where the resistivity of the soil is 100 times greater than that of the concrete. The percentage reduction in the resistance of the electrode appears to remain constant at around 47% (100 → 1000 Ω m).

Y L Chow [22] proposed the sunken grid in first layer of two-layer earth, the resistance, R_g, of a grid shown in Fig 6.12 is given by

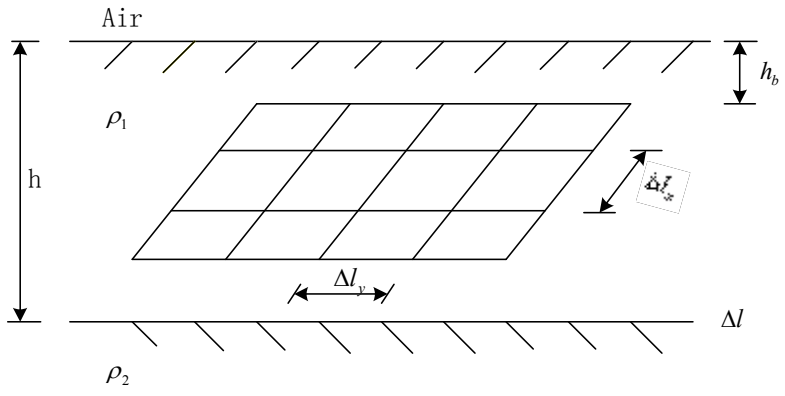

Fig 6.12 Grid in two-layer earth

$$R_g = \rho_1\left[\frac{1}{4}\sqrt{\frac{\pi}{A}} + \frac{1}{L}\left(\frac{1}{2\pi}\ln\frac{0.061\Delta l}{d_0}\right)\right]\cdot\left(1-\frac{2.256h_b}{\sqrt{A}}\right) - \rho_1\frac{\ln(1-K)}{2\pi(h+h_0)} \qquad (6.25)$$

Where $K = \dfrac{\rho_2 - \rho_1}{\rho_2 + \rho_1}$ (6.26)

$$h \prec 0.2\sqrt{A}, h_b \prec h$$

$$h_0 = c_f\sqrt{\frac{A}{2\pi}}[\ln(1-K)]\frac{K-1}{2K} \qquad (6.27)$$

$$\Delta l = \sqrt{\Delta l_x \cdot \Delta l_y} \qquad (6.28)$$

And

Δl_x The single mesh length in x directions (m)

Δl_y The single mesh length in y directions (m)

A The area of the grid (m^2)

ρ_1 The resistivity of the upper earth (Ω m)

ρ_2 The resistivity of the lower earth (Ω m)

d_0 The grid conductor diameter (m)

L The total length of grid conductors (m)

h_b The grid sunken depth below earth surface (m)

h The height of the upper earth layer (m)

c_f The area shape factor (≈ 0.9)

If we assume that the ρ_1 represents the resistivity of conductive concrete, the above formula can be used in the calculation of resistance of the concrete-encased earth electrodes.

6.3 Summary

The possible approaches for attenuating surges have been introduced. All the related models and the effect of soil resistivity have been presented.

In the approaches of surge attenuation, earthing plays a significant role. It is the ultimate solution to disperse the surge yielded on the distribution system.

When lightning current injected into electrodes exceeds a critical value, the soil surrounding the electrodes becomes ionized. Soil ionization is a particular phenomenon in the process of surge attenuation, and its impedance characteristic is different from the non-ionized soil characteristic. Lower soil resistivity implies that for ionization to take place a higher current density is needed.

A model of concentrated earth electrode was used to quantify the non-linear effect of soil ionization and soil resistivity. The effect of soil ionization shows a significant decrease in the effective resistance of a driven rod under surge conditions. This decrease is typically in the range of 20% to 80% of the low current resistance value. Soil ionization does not affect the performance of long trench electrodes, even if the trench electrodes are in the soil of high resistivities.

Three point star electrodes constructed by the combination of driven rods and buried trench conductors have excellent impedance performance for lightning discharge surges. Therefore three point star has been selected by ESKOM as the electrode configuration of distribution transformer.

Encasing an earth electrode in conductive concrete is a costly means of reducing the electrode resistance to true earth. However, it is a good solution for certain soil conditions in South Africa. For the domestic consumers who live in a building, it is better to use the foundation earth electrodes of a building as the earth electrodes. Encasing electrodes in concrete has the added benefit of improved resistance to theft. Conductive concrete is

less effective in more conductive soils and should not be used in the cases where the soil resistivity is less than 300 Ω m.

For very high frequencies, the impedance in most soil conditions will decrease with frequency increase. However, for lightning surge overvoltages with frequency below 1 MHz, high-frequency properties can only be expected to cause a notable decrease with high soil resistivity. Through examining the effect of soil resistivity on transmission line transients, it has been found that a 1% variation in soil resistivity can result in nearly 0.5% change in the attenuation of a surge.

Chapter 7

CONCLUSIONS

This research report focuses on the effect of soil resistivity on the LV surge environment. After carrying out this investigation from previously published experimental results and research results, the following conclusions can be drawn.

Surges in distribution systems are either internal overvoltages or external overvoltages. Power frequency temporary overvoltages are one of the internal overvoltages due mainly to ground faults. Lightning related overvoltages are the major external overvoltages. Lightning and temporary overvoltages are the major influence factors in distribution networks. Direct strikes have higher peak current and voltage magnitudes than indirect strikes; therefore direct strikes are often the cause of severe damage to power systems.

When calculating the return stroke horizontal electric fields, at very close distance (less than 200 m) from the lightning channel and for ground conductivities of about $10^{-2} S/m$ or higher, the perfect conducting ground assumption can be considered as reasonable for an observation point located at a few meters above ground.

The influence of the ground conductivity on the surge propagation along overhead lines depends obviously on the lines length. For lines whose length does not exceed a certain 'critical' value (typically 2 km), the surge propagation along the line is not appreciably affected by the ground finite conductivity which, therefore, can be neglected in the computation process of lightning-induced voltages. Magnitudes of lightning-induced voltages for an infinitely long line increase for lower ground conductivity due to the effect of this parameter on the horizontal electric field coupling with the line. The expected number of faults due to these overvoltages increases for lines located over low conductivity grounds.

Lightning surges occurring on MV distribution lines can be transferred down to LV consumers through distribution transformer. The model of the distribution transformers can be used for the calculation of surges. The transfer function is a good tool for quantifying the propagation of lightning surges through transformers. Typically, 50% of the amplitude of a lightning surge can be transferred through the transformer. Lightning surges exciting internal resonances can result in problems with transformers.

In the protection of distribution systems against lightning surges, surge arresters play a very important role.

If lightning strike the earth termination system of a building, and the earth impedance is low, most of the lightning current can flow to earth. However, if the earth impedance is large enough, the induced voltage between the earthing system and the electrical system inside the building could be large enough to cause insulation flashover, SPD operation or damage to unprotected equipments.

When lightning current surges injected into electrodes exceed a critical value, the soil surrounding the electrodes becomes ionized. Soil ionization is a particular phenomenon in the process of surge attenuation in the soil, and its impedance characteristic is different from the non-ionized soil characteristic. Lower soil resistivity implies that for ionization to take place a higher current density is needed. Increasing water content can decrease both E_0 (critical breakdown intensity) and the soil resistivity, however, no direct correlation exists between E_0 and the soil resistivity, because the soil resistivity is also dependent on the amount of salt in the soil. The effect of soil ionization shows a significant decrease in the effective resistance of a driven rod under surge conditions. This decrease is typically in the range of 20% to 80% of the low current resistance value.

The earthing resistance of an earth electrode depends on the earth resistivity as well as the electrode geometry. The resistivity of the soil surrounding an earth electrode has a significant impact on its resistance. Soil resistivity also has a bearing on the potential

gradients that are to be expected at the soil surface during times of fault current discharge through the earth electrode.

Due to the self-inductances of earth electrodes, the frequency-dependent properties and the ionization process of soil surrounding earth electrodes the impulse impedances of the earth electrodes can differ from their low-voltage power-frequency resistance values significantly. The earth electrodes exhibit different impedance characteristics for currents of different magnitudes and frequencies. Trench electrodes are known to offer lower impedance to power frequency than vertical conductors. Vertical rods offer superior performance under surge conditions. The curves for estimating the impedances of electrodes in response to lightning current waveshapes were derived empirically. At peak current, the decrease in the impedance of an electrode can seldom be expected to be more than 15%, unless conditions of exceptionally high resistivity prevail. In the approaches of surge dispersion, earthing plays a significant role. It is the ultimate solution to disperse the surge yielded on the distribution system.

Encasing earth electrodes in conductive concrete is a costly means of reducing electrode resistance to true earth. However, it is a good solution for certain soil conditions in South Africa. For the domestic consumers who live in a building, it is better to use the foundation earth electrodes of a building as the earth electrodes. They have the added benefit of avoidance of theft. Conductive concrete is less effective in more conductive soils and should not be used in the case where the soil resistivity is less than 300 Ω m.

For very high frequencies, the impedance in most soil conditions will well decrease with frequency increases. However, for lightning surge overvoltages with frequency below 1 MHz, high-frequency properties can only be expected to cause a notable decrease with high soil resistivity.

After having considered the above conclusions, it can be found that the resistance or the impedance didn't play a key role in the process of surge dispersion in the LV distribution system. In fact, from this research, the soil resistivity is the most essential factor that

affects surge generation, surge propagation and surge attenuation, even if there are other factors that are also important for dispersing the surge in the LV distribution system. The conclusions provided a considerable background theory to another project (serving for IEC 62305-2) that investigating the risk issues related to the surge environment in domestic premises.

REFERENCES AND BIBLIOGRAPHY

[1] SABS IEC 61643-1(1998), 'SABS IEC 61643-1: Surge Protection Devices Connected to Low-Voltage Power Distribution Systems: Part 1: Performance Requirements and Testing Methods', The South African Bureau of Standards. ISBN 0-626-11950-2.

[2] SABS IEC 1312-1(1995), 'SABS IEC 1312-1: Protection against Lightning Electromagnetic Impulse', The South African Bureau of Standards. ISBN 0-626-10627-3.

[3] SABS IEC 1024-1(1990), 'SABS IEC 1024-1: Protection of Structures against Lightning: Part 1: General Principles', The South African Bureau of Standards. ISBN 0-626-10223-5.

[4] SABS 0199(1985), 'SABS 0199-1985: Code of Practice for the Design and Installation of an Earth Electrode', South African Bureau of Standards. ISBN 0-626-07488-6.

[5] IEC 62305-2 (2005): Protection against Lightning - Part 2: Risk Management

[6] SABS 0292(1999), 'SABS 0292-1999: Code of Practice Earthing of Low-Voltage (LV) Distribution Systems', South African Bureau of Standards. ISBN 0-626-12006-3.

[7] SABS 0313(1999), 'SABS 0313-1999: Code of Practice the Protection of Structures against Lightning ', South African Bureau of Standards. ISBN 0-626-12104-3.

[8] ESKOM (1999), 'Distribution Standard Part 2: Earthing', ESKOM Distribution Standard.

[9] ESKOM (2001), 'MV and LV Reticulation Earthing', ESKOM Distribution Standard.

[10] Phil Crowdy (1996), 'Distribution Technical Bulletin'.

[11] N. Kokkinos & I. Cotton, 'Transient Behaviour of Low Voltage Distribution Systems', UMIST, Manchester.

[12] William. A. Chisholm & Wasyl. Janischewskyj (1989), 'Lightning Surge Response of Ground Electrodes', IEEE Transactions on Power Delivery, Vol. 4, No.2, pp. 1329-1337.

[13] Enrique E. Mombello (2002), 'Impedances for the Calculation of Electromagnetic Transients Within Transformers', IEEE Transactions on Power Delivery, Vol. 17, No.2, pp. 479-487.

[14] E. Hanique (1994), 'A Transfer Function is a Reliable Tool for Comparison of Full- and Chopped Lightning Impulse Tests', IEEE Transactions on Power Delivery, Vol. 9, No.3, pp. 1261-1266.

[15] Abdul. M. Mousa (1994), 'The Soil Ionization Gradient Associated with Discharge of High Currents into Concentrated Electrodes', IEEE Transactions on Power Delivery, Vol. 9, No.3, pp. 1669-11677.

[16] Adam Semlyen (2002), 'Accuracy Limit in the Computed Transients on Overhead Lines Due to Inaccurate Ground Return Modeling', IEEE Transactions on Power Delivery, Vol. 17, No.3, pp. 872-878.

[17] C. J. Blattner (1982), 'Study of Driven Ground Rods and Four Point Soil Resistivity Tests', IEEE Transactions on Power Apparatus and Systems, Vol. PAS-101, No.8, pp. 2837-2850.

[18] F. Dawalibi & W. G. Finney (1980), 'Transmission Line Tower Grounding Performance in Non-Uniform Soil', IEEE Transactions on Power Apparatus and Systems, Vol. PAS-99, No.2, pp. 471-479.

[19] E E Oettle (1988), 'A New General Estimation Curve for Predicting the Impulse Impedance of Concentrated Earth Electrodes', IEEE Transactions on Power Delivery, Vol. 3, No.4, pp. 2020-2029.

[20] Leonid Grcev & Farid Dawalibi (1990), 'An Electromagnetic Model for Transients in Grounding Systems', IEEE Transactions on Power Delivery, Vol. 5, No.4, pp. 1773-1780.

[21] Carlos T. Mata, Mark I. Fernandez, Vladimir A. Rakov, Martin A. Uman (2000), 'EMTP Modeling of a Triggered-Lightning Strike to the Phase Conductor of an Overhead Distribution Line', IEEE Transactions on Power Delivery, Vol. 15, No.4, pp. 1175-1181.

[22] Y L Chow, M M Elsherbiny, M M A Salama (1996), 'Resistance Formulas of Grounding Systems in Two-Layer Earth', IEEE Transactions on Power Delivery, Vol. 11, No.3, pp. 1330-1336.

[23] C. J. Blattner (1980), 'Prediction of Soil Resistivity and Ground Rod Resistance for Deep Ground Electrodes', IEEE Transactions on Power Apparatus and Systems, Vol. PAS-99, No.5, pp. 1758-1763.

[24] J. R. Carson (1926), 'Wave Propagation in Overhead Wires with Ground Return', Bell Syst. Tech. j. vol. 5, pp.539-554.

[25] R.Velazquez & D. Mukhedkar (1984), 'Analytical Modelling of Grounding Electrodes Transient Behavior', IEEE Transactions on Power Apparatus and Systems, Vol. PAS-103, No.6, pp. 1314-1321.

[26] Carlo Mazzetti & Giuseppe M. Veca (1983), 'Impulse Behavior of Ground Electrodes', IEEE Transactions on Power Apparatus and Systems, Vol. PAS-102, No.9, pp. 3148-3155.

[27] T. Takashima, T. Nakae, R. Ishibashi (1981), 'High Frequency Characteristics of Impedances to Ground and Field Distributions of Ground Electrodes', IEEE Transactions on Power Apparatus and Systems, Vol. PAS-100, No.4, pp. 1893-1899.

[28] P. T. M. Vaessen & E. Hanique (1992), 'A New Frequency Response Analysis Method for Power Transformers', IEEE Transactions on Power Delivery, Vol. 7, No.1, pp. 384-389.

[29] Beutel, Andreas Alan (2000), The Application of Silicon Avalanche Devices for the Protection of Low Voltage Equipment from Dangerous Transients, Master's Research Report, University of the Witwatersrand.

[30] Oettle, E. E. (1987), The Impulse Impedence of Concentrated Earth Electrodes, Master's Research Report, University of the Witwatersrand.

[31] Nixon, Kenneth John (1999), Modeling the Lightning Transient Response of an Earth Electrode System, Master's Research Report, University of the Witwatersrand.

[32] Nixon, K. J, JM Van Coller, IR Jandrell (2004), 'Earthing and Lightning Protection REV. 1.0', University of the Witwatersrand.

[33] Power Quality Application Guide, 'A Systems Approach to Earthing', Copper Development Association.

[34] Power Quality Application Guide, 'Earthing Systems – Fundamentals of Calculation and Design', Copper Development Association.

[35] Rhett Alexander Kelly (1996), Lightning Surge Propagation from Medium Voltage to Low Voltage Power Distribution Networks, Master's Research Report, University of the Witwatersrand.

[36] JM Van Coller (2004), 'Insulation Coordination', University of the Witwatersrand.

[37] Arshad Mansoor & Francois Martzloff (1998), 'The Effect of Neutral Earthing Practices on Lightning Current Dispersion in a Low-Voltage Instllation', IEEE Transactions on Power Delivery, Vol. 13, No.3, pp. 783-790.

[38] Ronald P. O'Riley (1990), *Electrical Grounding*, Delmar Publishers, Inc. pp. 29-31.

[39] IEEE Std 142-1972 (1972), 'IEEE Recommended Practice for Grounding of Industrial and Commercial Power Systems', The Institute of Electrical and Electronics Engineers, Inc.

[40] Nixon, K. J, I.R Jandrell, 'Quantifying the Lightning Transient Performance of an Earth Electrode', University of the Witwatersrand.

[41] Dan Mordechai Eytani (1995), Earthing Electrodes-Power Frequency and Impulse Behaviour, Master's Research Report, University of the Witwatersrand.

[42] Darryl Chapman (1999), An Investigation into the Modeling and Testing of Conductive Concrete for Use in Earthing Applications, Master's Research Report, University of the Witwatersrand.

[43] Liew, A. C. & Darveniza, M. (1974), 'Danamic Model of Impulse Characteristics of Concentrated Earths', Proceedings of the IEE, Vol. 121, No.2, pp. 123-135.

[44] Korsuncev, A.V.(1958), 'Application on the Theory of Similarity to Calculation of Impulse Characteristics of Concentrated Electrodes', Elektrichestvo, No.5, pp. 31-35.

[45] SABS IEC 1024-1-1 (1993), 'Protection of Structures against Lightning: Part 1: General Principles', The South African Bureau of Standards. ISBN 0-626-10287-1.

[46] R. Rudenberg. (1945) "Grounding Principles and Practices Ⅰ- Fundamental Considerations on Ground Currents", Electrical Engineering, Vol.64, January, pp. 1-13.

[47] Farhad Rachidi, Carlo Alberto Nucci, Michel Ianoz and Carlo Mazzetti (1996), 'Influence of a Lossy Ground on Lightning-Induced Voltages on Overhead Lines', IEEE Transactions on Electromagnetic Compatibility, Vol. 40, No.4, pp. 250-263.

[48] Veron Cooray and Viktor Scuka (1998), 'Lightning-Induced Overvoltages in Power Lines: Validity of Various Approximations Made in Overvoltage Calculations', IEEE Transactions on Electromagnetic Compatibility, Vol. 40, No.4, pp. 355-363.

[49] Victor F. Hermosillo and Vernon Cooray (1995), 'Calculation of Fault Rates of Overhead Power Distribution Lines Due to Lightning-Induced Voltages Including the Effect of Ground Conductivity', IEEE Transactions on Electromagnetic Compatibility, Vol. 37, No.3, pp. 392-398.

[50] J. Zenneck, *Wireless Telegraphy*. New York: McGraw Hill, English Translation by A. E. Seelig, 1915.

[51] V. Cooray, “Horizontal Fields Generated by Return Strokes,” Radio Sci. vol. 27, pp. 529-537, July-Aug. 1992.

[52] M. Rubinstein (1996), ‘An Approximate Formula for the Calculation of the Horizontal Electric Field from Lightning at Close, Intermediate and Long Ranges’, IEEE Transactions on Electromagnetic Compatibility, Vol. 38. No.3, pp.531-535.

[53] F. Rachidi, M. Ianoz, C. A. Nucci, and C. Mazzetti, “Calculation Methods of the Horizontal Component of Lightning Return Stroke Electric Fields,” in Int. Wroclaw Symp. Electromag. Compat, Wroclaw, Sept. 1992.

[54] A.K. Agrawal, H.J.Price, and S. H. Gurbaxani, (1980), ‘Transient Response of Multiconductor Transmission Lines Excited by a Nonuniform Electromagnetic Field’, IEEE Transactions on Electromagnetic Compatibility, Vol EMC-22, pp. 119-129.

[55] E.D. Sunde, *Earth Conduction Effects in Transmission Systems*. New York: Dover, 1968.

[56] C.Cary, “Approche Complte de la Propagation Multifilaire en Haute Frequence par l’utilization des Matrices Complexes, *EDF Bulletin de la direction des etudes er recherches, Serie B*, no. 3/4, pp. 5-20, 1976.

[57] E. F. Vance, Coupling to Shielded Cables. New York: Wiley Interscience, 1978.

[58] K. C. Chen and K. M. Damrau (1989), ‘Accuracy of Approximate Transmission Line Formulas for Overhead Wires’, IEEE Transactions on Electromagnetic Compatibility, Vol 31, pp. 396-397.

[59] Dale Shoup (1992), ‘Sensors in the Real World’.